

AD-A073 229

MASSACHUSETTS INST OF TECH LEXINGTON LINCOLN LAB
AIR TRAFFIC DENSITY AND DISTRIBUTION MEASUREMENTS. (U)
MAY 79 W H HARMAN

F/G 1/2

UNCLASSIFIED

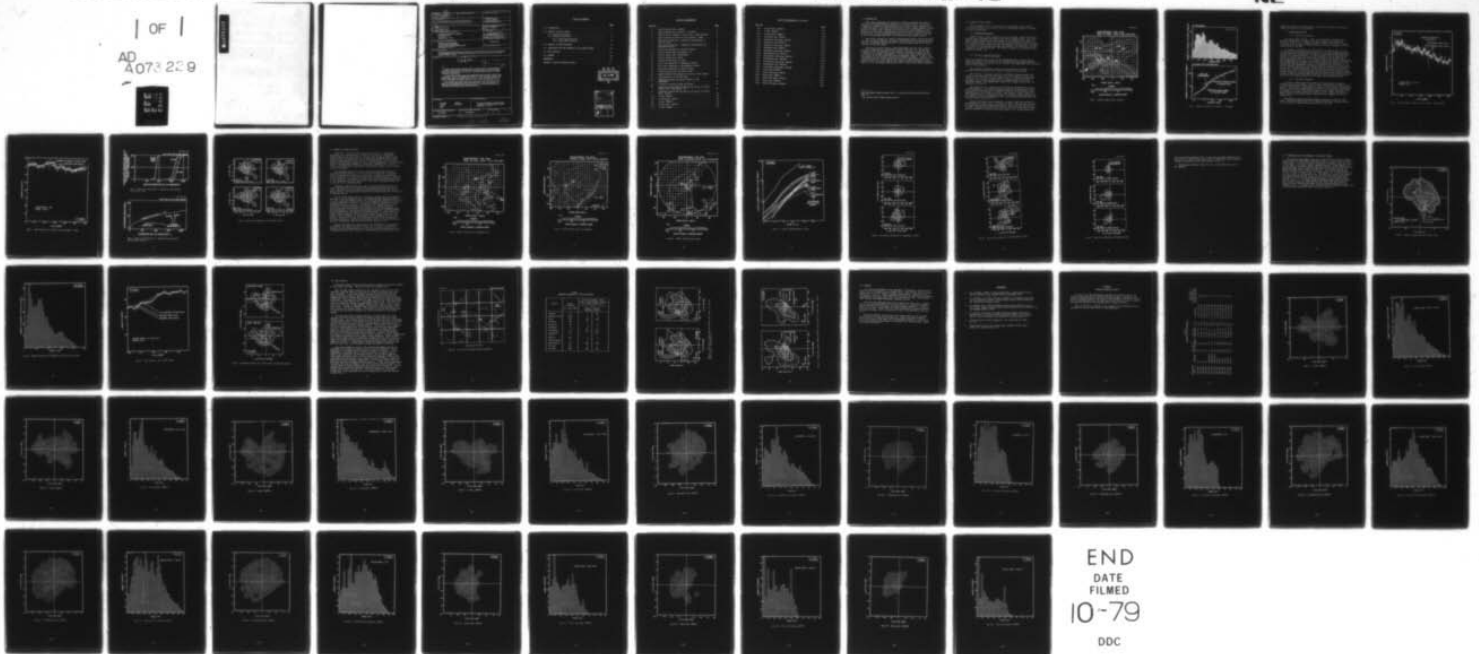
ATC-80

FAA-RD-78-45

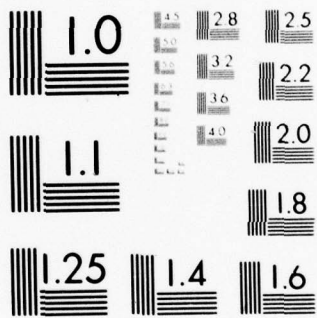
DOT-FA77WAI-817

NL

| of |
AD
A073 229
1



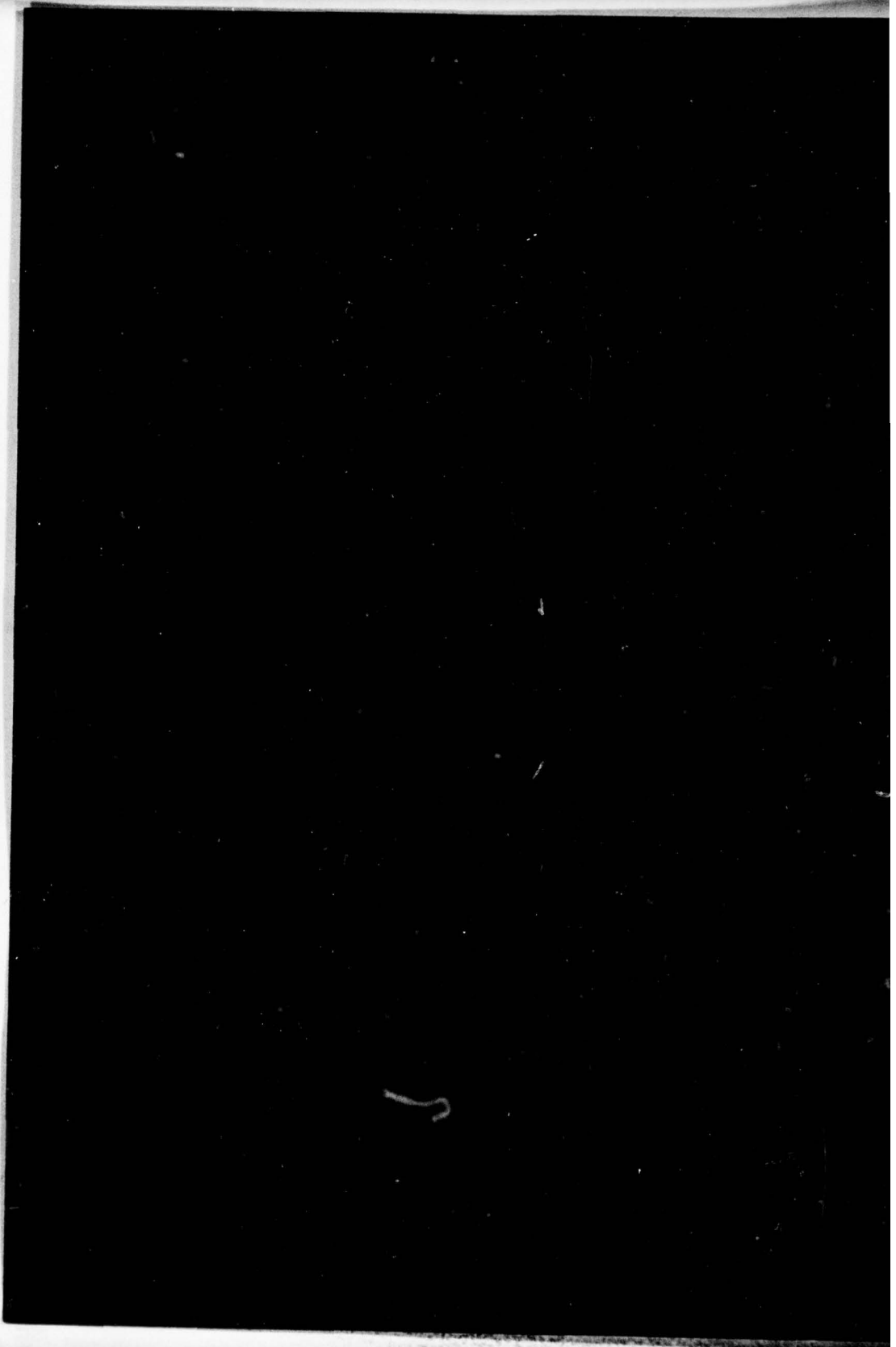
END
DATE
FILMED
10-79
DDC



MICROCOPY RESOLUTION TEST CHART
 NATIONAL BUREAU OF STANDARDS-1963-A

MA073229

A



1. Report No. 18 FAA-RD-78-45		2. Government Accession No.		3. Recipient's Catalog No.	
4. Title and Subtitle 6 Air Traffic Density and Distribution Measurements				5. Report Date 11 3 May 79	
7. Author(s) 10 W.H. Harman				8. Performing Organization Report No. 14 ATC-80	
9. Performing Organization Name and Address Massachusetts Institute of Technology Lincoln Laboratory P.O. Box 73 Lexington, MA 02173				10. Work Unit No. Proj. No. 052-241-04	
12. Sponsoring Agency Name and Address Department of Transportation Federal Aviation Administration Systems Research and Development Service Washington, DC 20591				11. Contract or Grant No. 15 DOT-FA77-WAI-817	
15. Supplementary Notes The work reported in this document was performed at Lincoln Laboratory, a center for research operated by Massachusetts Institute of Technology, with the support of the Department of the Air Force under Contract F19628-78-C-0002.				13. Type of Report and Period Covered Project Report	
16. Abstract 12 61p. 9 Project repty. Results of measurements to determine peak air traffic densities, the spatial distribution of air traffic, and its variation with time, in the Los Angeles Basin and at several locations from Boston to Washington, D.C. are reported. These measurements include only ATCRBS-transponder equipped aircraft. LA Basin traffic densities are shown to be significantly higher than those measured at any other location. The time- and spatial-average density over a circular region of 10 nmi radius reaches a peak value of 0.1 aircraft per sq. nmi in LA. Under comparable conditions the density in Washington, Philadelphia, and Boston reaches 0.02 to 0.04 aircraft per sq. nmi. These measurements, made in 1976, were compared with the LA Basin Standard Traffic Model as to spatial distribution of traffic and absolute density. The results show that the model and the measurement differ by a scale factor of 5:1 (with density being greater in the model) but otherwise agree closely in spatial distribution.					
17. Key Words Air traffic ATCRBS DABS BCAS LA Basin Interference			18. Distribution Statement Document is available to the public through the National Technical Information Service, Springfield, VA 22151		
19. Security Classif. (of this report) Unclassified		20. Security Classif. (of this page) Unclassified		21. No. of Pages 64	

207 650

GW

TABLE OF CONTENTS

	<u>Page</u>
1.0 INTRODUCTION	1
2.0 TRAFFIC IN THE LA BASIN	2
2.1 Spatial Distribution	2
2.2 Variation with Time	5
2.2.1 Short-Term Variation	5
2.2.2 Day-to-Day Variation	5
3.0 TRAFFIC IN OTHER LOCATIONS	10
4.0 COMPARISON WITH THE STANDARD LA HIGH DENSITY MODEL	19
5.0 DATA VALIDITY	24
6.0 SUMMARY	29
REFERENCES	30
APPENDIX DETAILED COMPUTER OUTPUTS	A-1

DDC
RECEIVED
 AUG 28 1979
RECEIVED
B

ACCESSION for		
NTIS	Write Section	<input checked="" type="checkbox"/>
DDC	Buff Section	<input type="checkbox"/>
UNANNOUNCED		<input type="checkbox"/>
JUSTIFICATION _____		
BY _____		
DISTRIBUTION/AVAILABILITY CODES		
Dist.	AVAIL. and/or	SPECIAL
A		

LIST OF ILLUSTRATIONS

<u>Fig. No.</u>		<u>Page</u>
1	Traffic Density Map, LA Basin	3
2	Range Distribution of Traffic -- LA Basin	4
3	Time Variation, Traffic in the LA Area - Peak Location	6
4	Time Variation of Traffic in the LA Basin - Total	7
5	Short Term Variability - Cumulative Distribution of Aircraft Count	8
6	Short Term Variability - Comparison Between Mean and Standard Deviation	8
7	Day-to-Day Comparison of LA Basin Traffic	9
8	Traffic Density Map, Washington, D.C.	11
9	Traffic Density Map, Philadelphia	12
10	Traffic Density Map, Boston	13
11	Traffic Distributions in Range	14
12	Day-to-Day Comparison of Washington Traffic	15
13	Day-to-Day Comparison of Philadelphia Traffic	16
14	Day-to-Day Comparison of Boston Traffic	17
15	Traffic Density Map, LAl Traffic Model	20
16	Range Distribution Histogram for the LAl Traffic Model.	21
17	Time Variation, LAl Traffic Model	22
18	Comparison Between LAl Traffic Model and TMF Measurement	23
19	X-Y Plot of Aircraft Tracks (LA Basin)	25
20	Comparison Between TMF and ARTS as the Source of Traffic Density Data - Washington, D.C.	27
21	Comparison Between TMF and ARTS as the Source of Traffic Data - Boston	28
A-1	LA Map, TMF8126	A-3
A-2	LA Histogram, TMF8126	A-4
A-3	LA Mpa, TMF8122	A-5
A-4	LA Histogram, TMF8122	A-6
A-5	LA Map, TMF8046	A-7

LIST OF ILLUSTRATIONS (Continued)

<u>Fig. No.</u>		<u>Page</u>
A-6	LA Histogram, TMF8046	A-8
A-7	LA Map, TMF8055	A-9
A-8	LA Histogram, TMF8055	A-10
A-9	Washington Map, TMF4039	A-11
A-10	Washington Histogram, TMF4039	A-12
A-11	Washington Map, TMF4001	A-13
A-12	Washington Histogram, TMF4001	A-14
A-13	Washington Map, TMF4054	A-15
A-14	Washington Histogram, TMF4054	A-16
A-15	Philadelphia Map, TMF5139	A-17
A-16	Philadelphia Histogram, TMF5139	A-18
A-17	Philadelphia Map, TMF5026	A-19
A-18	Philadelphia Histogram, TMF5026	A-20
A-19	Philadelphia Map, TMF5005	A-21
A-20	Philadelphia Histogram, TMF5005	A-22
A-21	Boston Map, TMF3031	A-23
A-22	Boston Histogram, TMF3031	A-24
A-23	Boston Map, TMF3037	A-25
A-24	Boston Histogram, TMF3037	A-26
A-25	Boston Map, TMF3008	A-27
A-26	Boston Histogram, TMF3008	A-28

1.0 INTRODUCTION

This report summarizes the results of a study to determine air traffic densities at several important locations in the United States. This type of information is needed in the development of air traffic control systems such as DABS and BCAS*. The design and evaluation of these systems depend on traffic density in several ways: computer track files must be large enough to accommodate all of the traffic encountered, and the tolerance to interference must be sufficient to permit undegraded operation even in the presence of the high levels of interference which are to be expected in high traffic density.

This report presents the results of measurements made in 1976 to determine the peak air traffic density, its spatial distribution, and its variation with time for transponder equipped aircraft in the Los Angeles area and at several locations on the East Coast.

The primary facility used for these measurements was the M.I.T. Lincoln Laboratory Transportable Measurements Facility (TMF, Ref. 3). The TMF was originally built and operated for the purpose of testing the design of DABS in realistic air traffic environments. During these tests it was found that the quality of the TMF surveillance data was markedly superior to that of the data produced by the currently operational ATRBS** equipment. Aircraft tracks in TMF were seen to be more uniform and regular: having significantly fewer missed reports, and having significantly improved range and azimuth accuracies (Ref. 4). For this reason, TMF data was used in this traffic density analysis.

* Discrete Address Beacon System (Ref. 1); Beacon Collision Avoidance System (Ref. 2).

** Air Traffic Control Radar Beacon System.

2.0 TRAFFIC IN THE LA BASIN

The Los Angeles Basin is reputed to have the highest traffic density in the United States. As a result, there is considerable interest in current LA traffic measurements.

2.1 Spatial Distribution

Figure 1 shows a traffic density map of the LA Basin. These results were obtained from a 20 minute recording of TMF data in November 1976. Each alphanumeric symbol represents the time average of the traffic density within 10 nmi of that location. That is, the aircraft located within a circle of radius $R = 10$ nmi were counted, and that count averaged over the duration of the sample (here 20 min.); this average count was then divided by the area πR^2 to obtain a density ρ in aircraft per nmi^2 . The result is shown via a logarithmic scale defined as follows. Let

$$\rho^* = 10 \log_{10} \frac{\rho}{0.001 \text{ aircraft/nmi}^2}$$

Then ρ^* is converted into an integer by dropping any digits to the right of the decimal point. That integer is then represented by an alphabet-extended decimal system where A = 10, B = 11, C = 12, etc. The logarithmic scale is marked in Fig. 1 for reference.

The counting of aircraft is based on target reports and tracks. A target report which correlates with a track is counted as one aircraft.

When the Fig. 1 data were recorded, the TMF was located at Brea, California on a prominent hilltop radar site about 20 nmi inland from the coast (33.96° N. Lat., 117.91° W. Long., 1400 ft. elev.). This site affords good coverage of the LA Basin including the San Fernando Valley and the San Bernardino region. Measurements which assess the coverage of this site are discussed in Section 5.

The results in Fig. 1 indicate that the spatial distribution of traffic is very nonuniform. As would be expected, densities are much lower over the ocean than over the land, and are relatively low over the mountainous region beginning about 15 nmi north of the TMF. Peak density is seen to occur in the Long Beach area. Although not as dense as the peak, local concentrations are apparent in the Van Nuys/Burbank area, in the Ontario/Riverside area, and along the coast southeast of LA.

Figure 2 shows the range distribution of traffic about the location of maximum density, namely $(X, Y) = (-10 \text{ nmi}, -10 \text{ nmi})$. This plot also includes for comparison two simple mathematical models, uniform-in-area and uniform-in-range. Comparisons indicate that within 10 nmi, the LA data may be approximately described as uniform-in-area with density of 0.1 aircraft/ nmi^2 , and

MEASUREMENT TMF 8126
 SUN. 21 NOV., 1978 11:30-11:50 PST

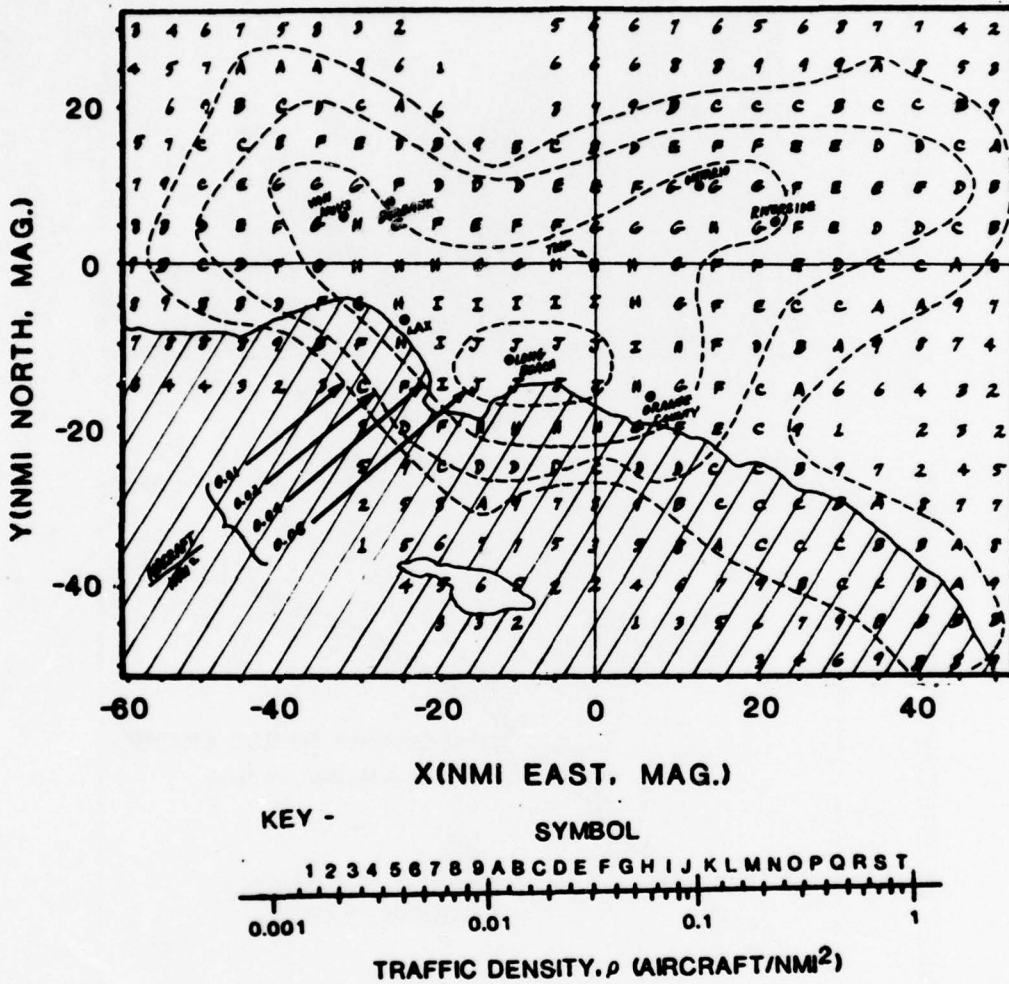


Fig.1. Traffic density map, LA Basin

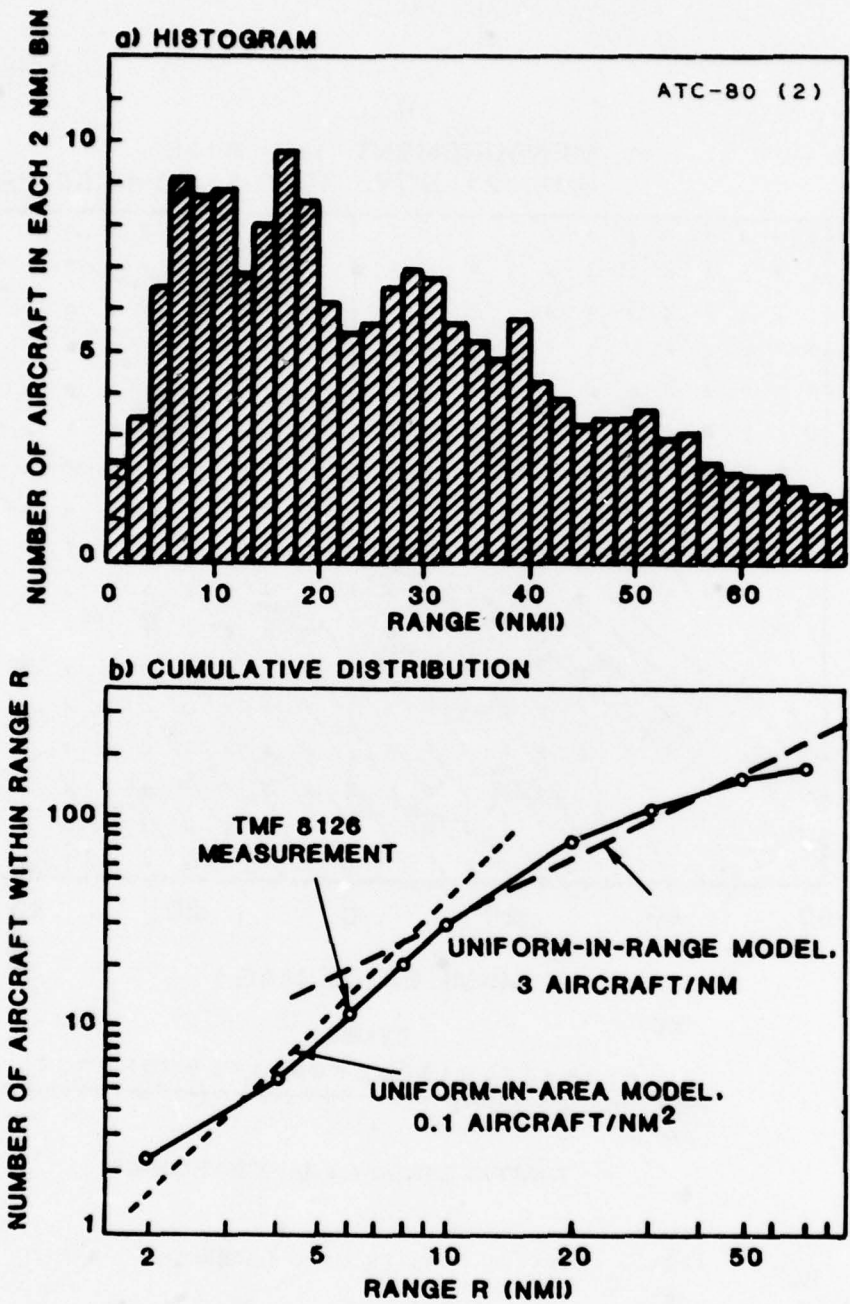


Fig.2. Range distribution of traffic -- LA Basin

between 10 and 50 nmi the data may be approximately described as uniform-in-range with density of 3 aircraft/nmi.

2.2 Variation with Time

2.2.1 Short-Term Variation

The results shown in Figs. 1 and 2 were obtained by averaging over a period of 20 minutes. Variations with time throughout that period are plotted in Figs. 3 and 4. Figure 3 pertains to the traffic within a range of 10 nmi of the location of highest density, and Fig. 4 includes all traffic within 80 nmi of the TMF.

The amount of variability in aircraft count is shown in Fig. 5 in the form of the cumulative distribution and in Fig. 6 as the standard deviation. It might have been expected that the amount of variability would agree approximately with Poisson statistics. In the "gas model" used to represent air traffic in certain cases, the probability distribution of aircraft count within any region is Poisson. For a random variable with Poisson distribution, the standard deviation is equal to the square root of the average value (Ref. 5). This relationship is plotted in Fig. 6 for comparison with the data. It is evident that the measurements conform to the Poisson law to first order, and yet the standard deviation of the measured data is consistently less than this simple rule. Possible mechanisms for this difference are (1) the structure of air traffic due to ATC and (2) the shortness of the sample (20 min.) which, because of the fact that it takes about 10 to 60 minutes for individual aircraft to pass through the counting region, generally tends to decrease the standard deviation of the sample relative to the longer term standard deviation.

2.2.2 Day-to-Day Variation

In order to assess day-to-day variation, TMF data tapes recorded on different days were processed. Figure 7 shows a comparison of LA Basin results on four different days. Although not all identical, the results are seen to be similar. The primary features mentioned above in connection with tape TMF8126 (low density over ocean and mountains, peak occurring around Long Beach, etc.) are evident in the other three day's traffic as well. TMF8126 recorded on a Sunday, exhibits the highest density among these four samples, but not by a large factor.

The Appendix gives more detailed computer outputs for these four TMF tapes. The traffic density map and the range distribution histogram centered at the location of highest density are given for each case.

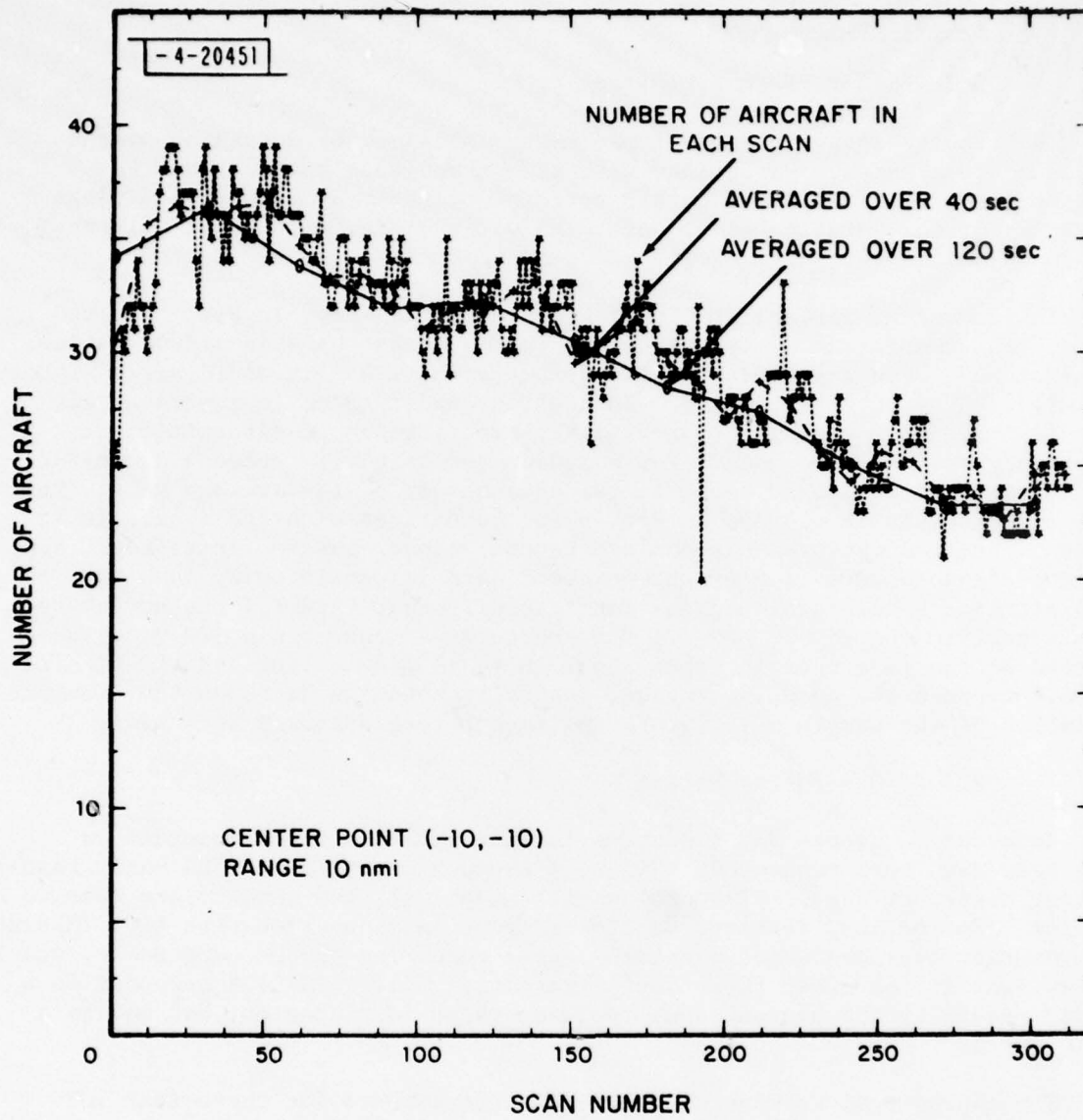


Fig.3. Time variation, traffic in the LA area - peak location

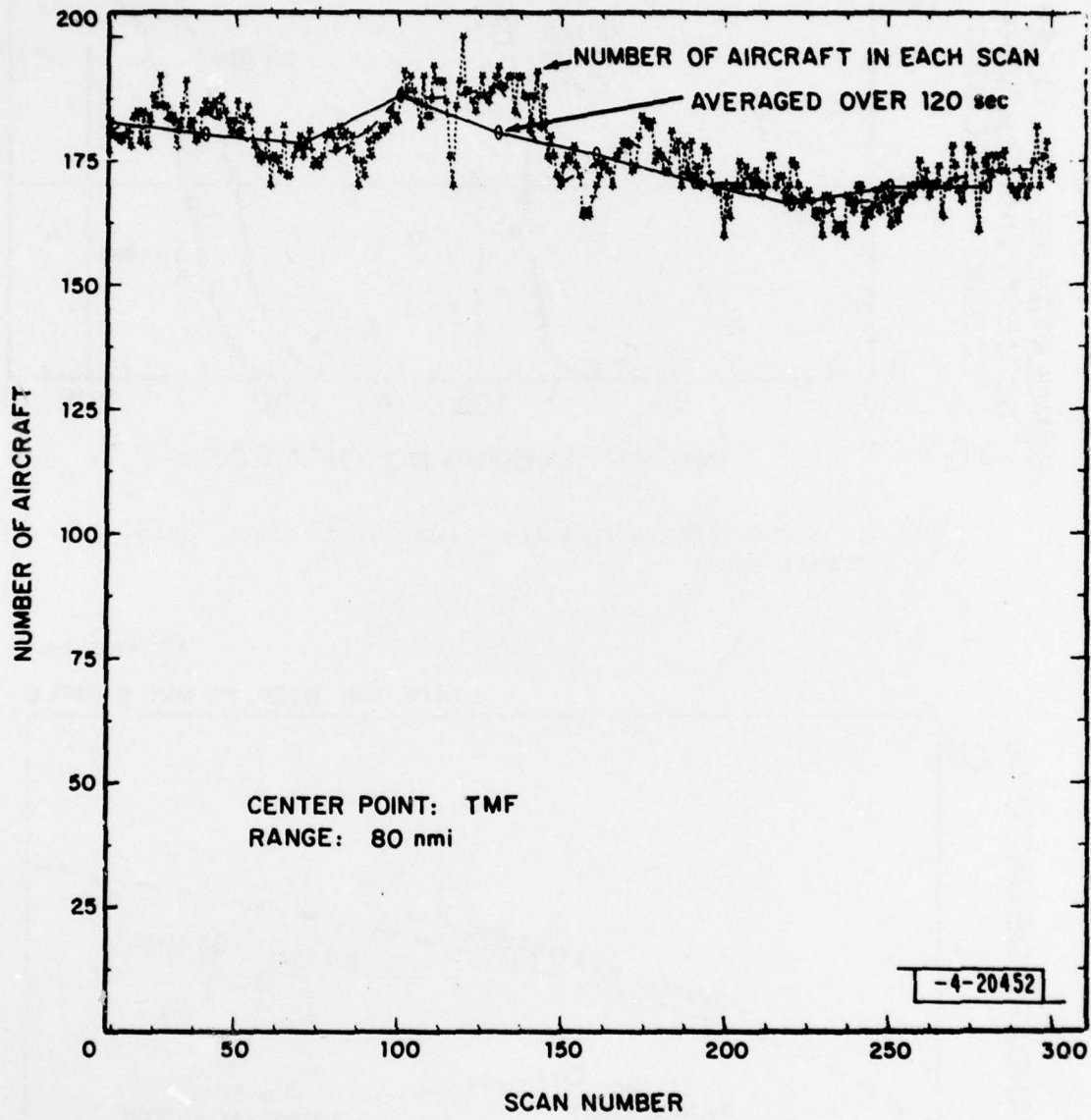


Fig.4. Time variation of traffic in the LA Basin - Total

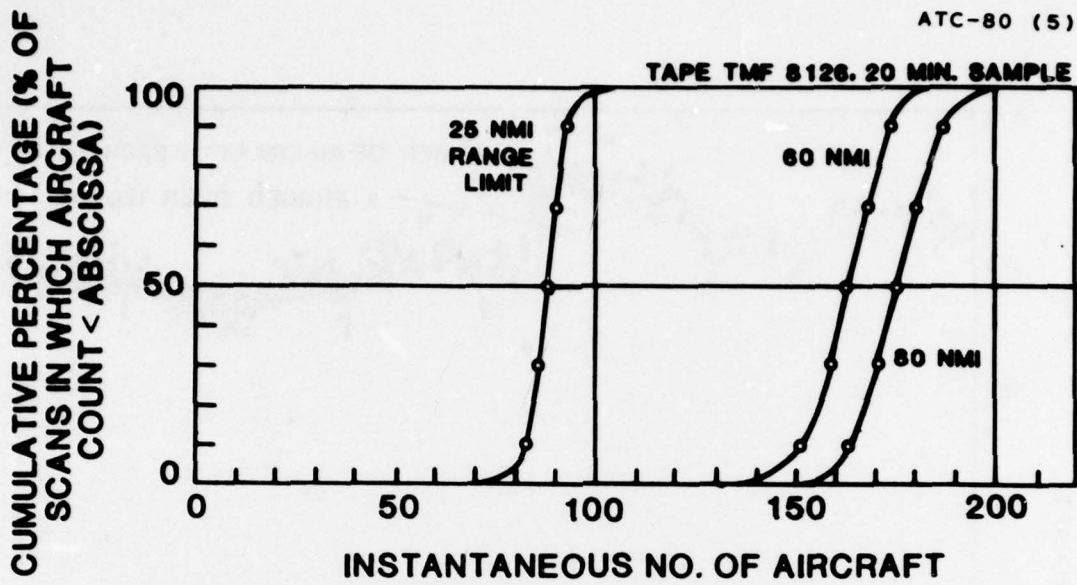


Fig.5. Short term variability - Cumulative distribution of aircraft count

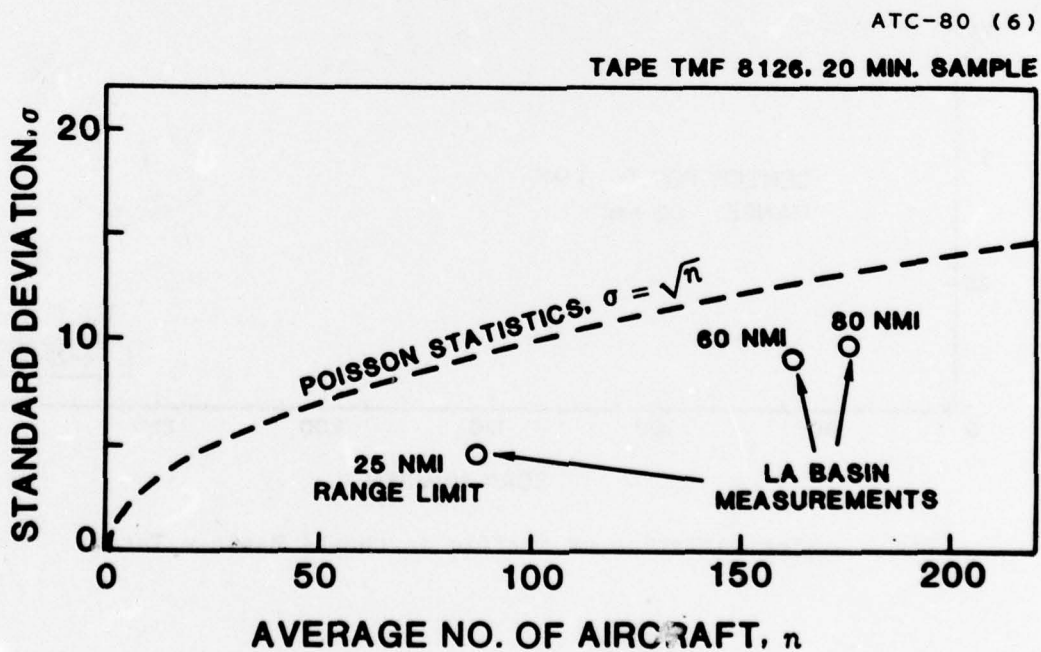


Fig.6. Short term variability - Comparison between mean and standard deviation

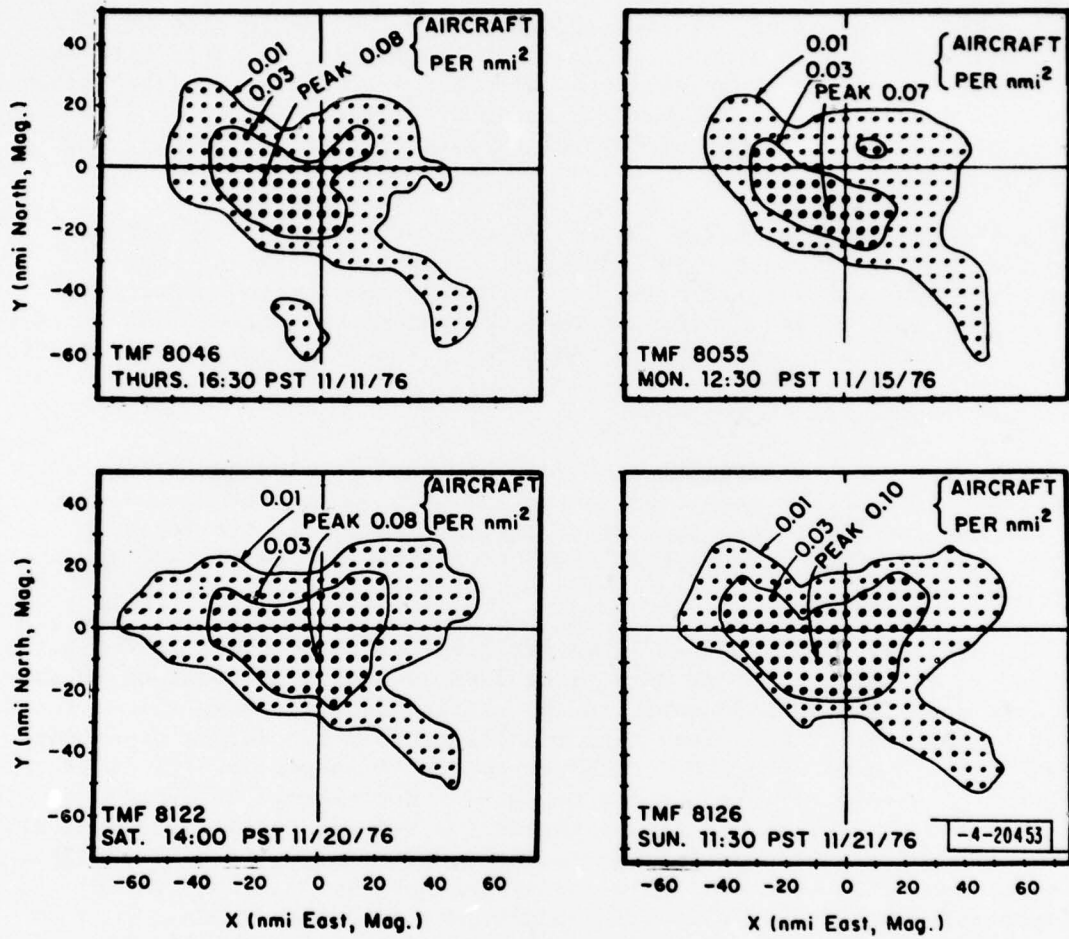


Fig.7. Day-to-day comparison of LA Basin traffic

3.0 TRAFFIC IN OTHER LOCATIONS

Figures 8, 9, and 10 present traffic density maps of, respectively, Washington, D.C., Philadelphia, and Boston. As in Fig. 1, the symbols plotted indicate the local density, averaged over the region within 10 nmi of each point. The Boston data was recorded with the TMF located at Deer Island, a favorable site about 2 nmi east of Logan Airport. This site was found to give excellent coverage of the airspace around Boston. The Philadelphia data was recorded when the TMF was located near Clementon, N.J., a site about 15 nmi southeast of Philadelphia International Airport also providing excellent coverage.

The Washington data in Fig. 8 was recorded with the TMF located at Washington National Airport. In this case it was found that an excessive number of targets were recorded at close range -- thought to be primarily false targets due to reflections and imperfect sidelobe suppression. Because of this condition, all targets with ranges less than 2 nmi were deleted prior to the computation of traffic densities. This range filtering was done only in the case of the Washington data.

Cumulative range distributions, $N(R)$, of aircraft plotted in Fig. 11 permit comparisons to be made among sites and among different days at each site. Each curve gives the range distribution relative to the location of maximum density. The curve marked "high density traffic model LA1" is discussed in the next section.

The day-to-day similarities in LA traffic, discussed above in connection with Fig. 7, are also apparent here, with TMF8126 having the maximum density. It is also seen that TMF8126 exhibits the maximum density among all of the tapes reduced, regardless of location. The results exhibit a moderate day-to-day repeatability in each location. Although the curve shapes in Fig. 11 are all similar, certain differences may be noted. For example $N(10 \text{ nmi})$ results at Boston, Philadelphia, and Washington are all approximately equal, and yet $N(60 \text{ nmi})$ results exhibit appreciable differences, with Philadelphia exceeding Washington, and Washington exceeding Boston. In other words, the traffic density in Boston falls off rapidly away from the location of peak density, while Washington and Philadelphia traffic densities fall off less rapidly. In all three cases, the distribution beyond 10 nmi is moderately well approximated by a uniform-in-range model, with 1 to 2 aircraft per nmi (which is considerably less than the 3 aircraft per nmi of LA).

Density map comparisons showing day-to-day repeatability to Washington, Philadelphia, and Boston are given in Figs. 12, 13, and 14. Day-to-day changes in spatial distribution are more evident in the Philadelphia plots as compared with the other locations. These changes may be the result of the

MEASUREMENT TMF 4039
 MON. 24 MAY, 1976, 11:14-11:34 EDT

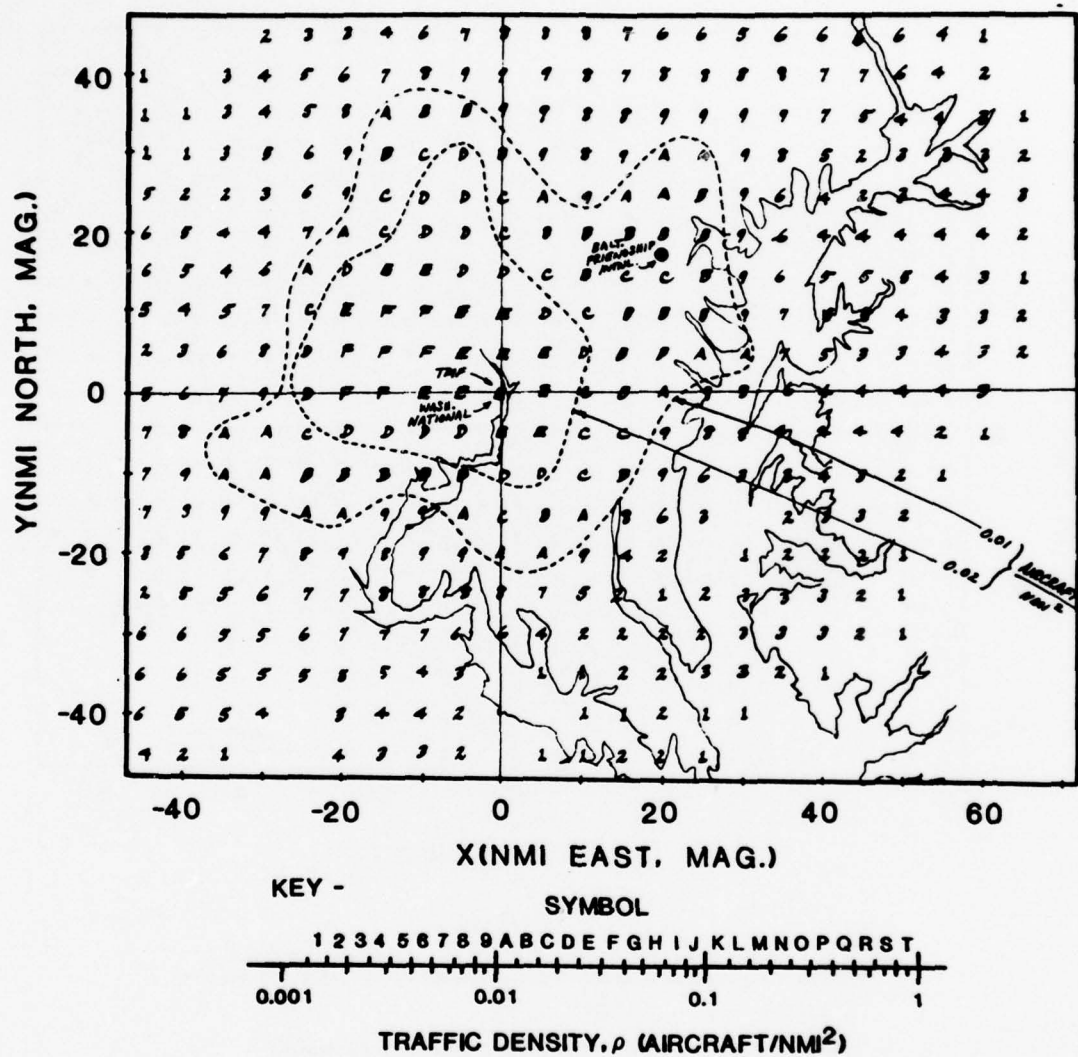


Fig.8. Traffic density map, Washington, D.C.

MEASUREMENT TMF 5026
THURS. 24 JUNE. 1976 13:58-14:28 EDT

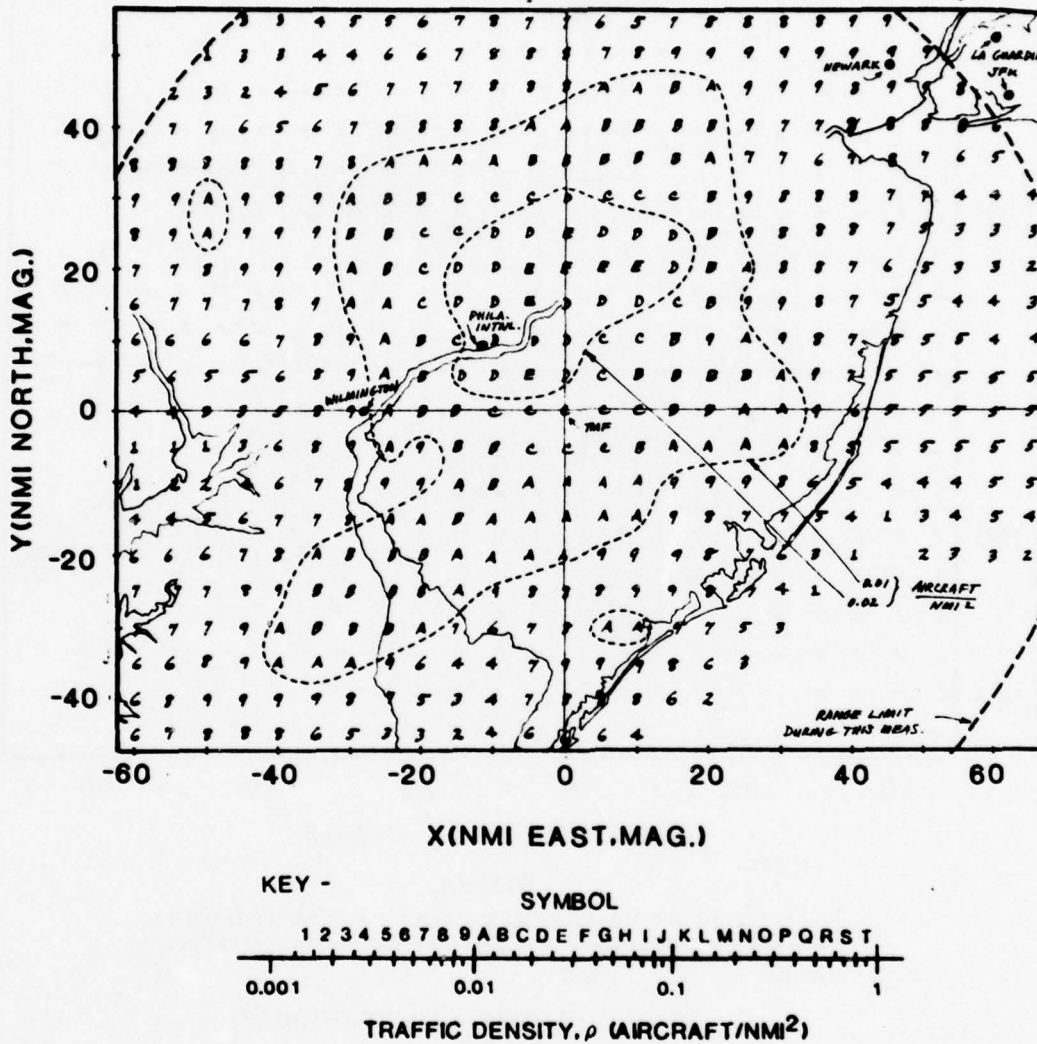


Fig.9. Traffic density map, Philadelphia

MEASUREMENT TMF 3037
 MON. 29 MARCH, 1976, 15:41-15:59 EST

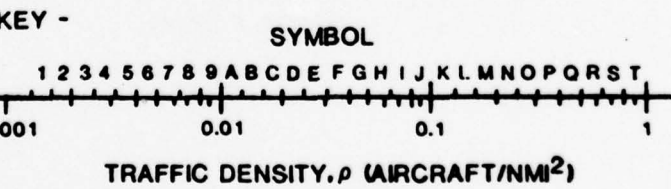
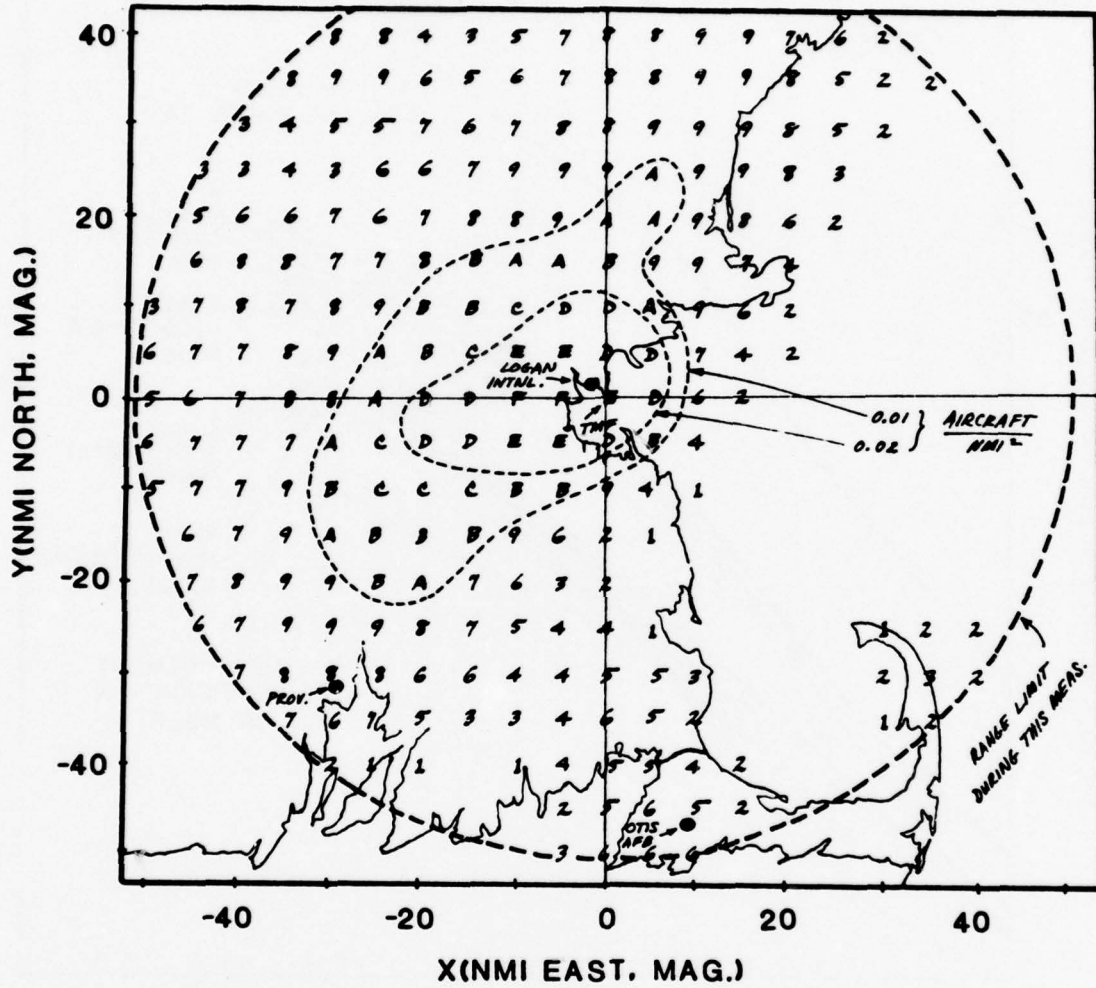


Fig.10. Traffic density map, Boston

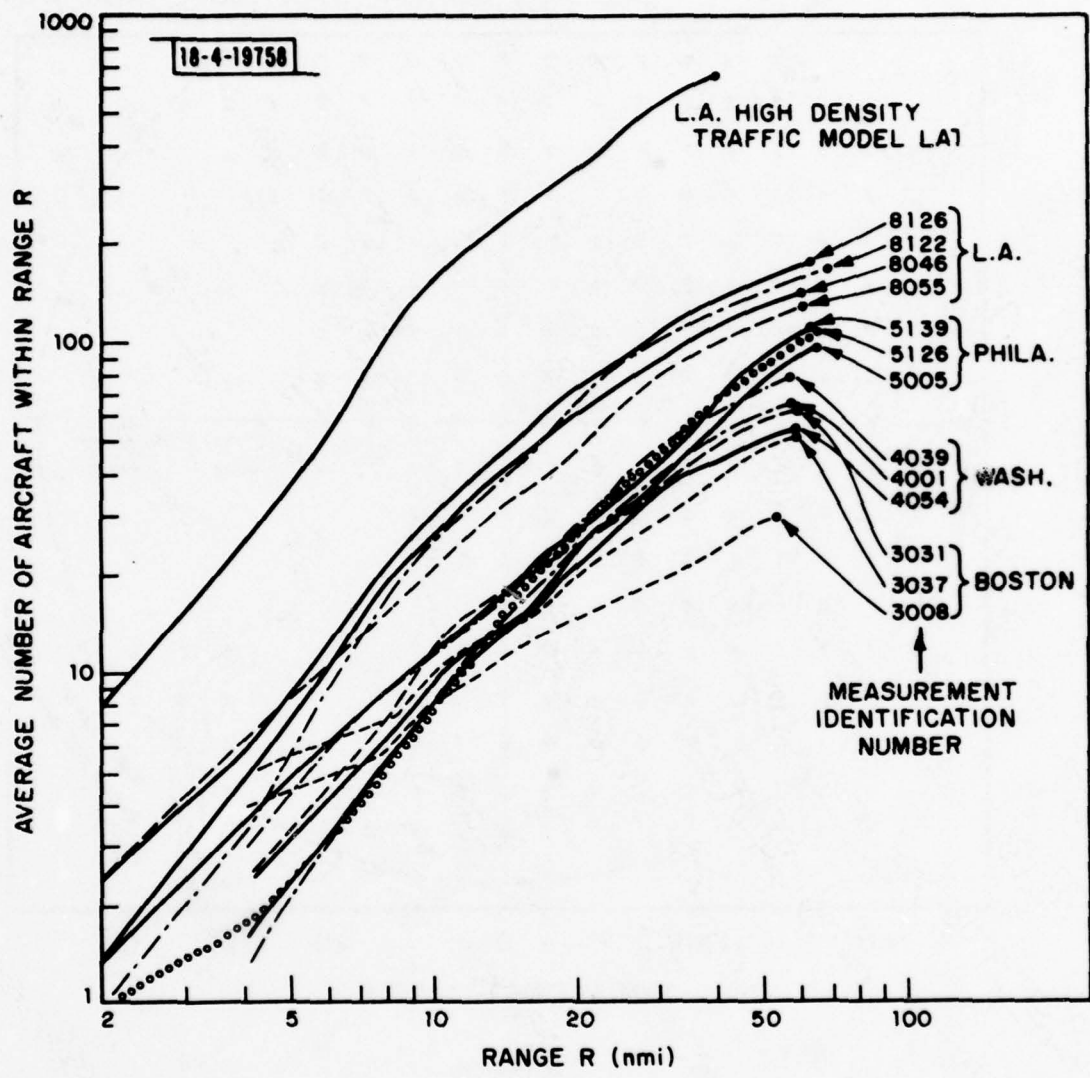


Fig.11. Traffic distributions in range

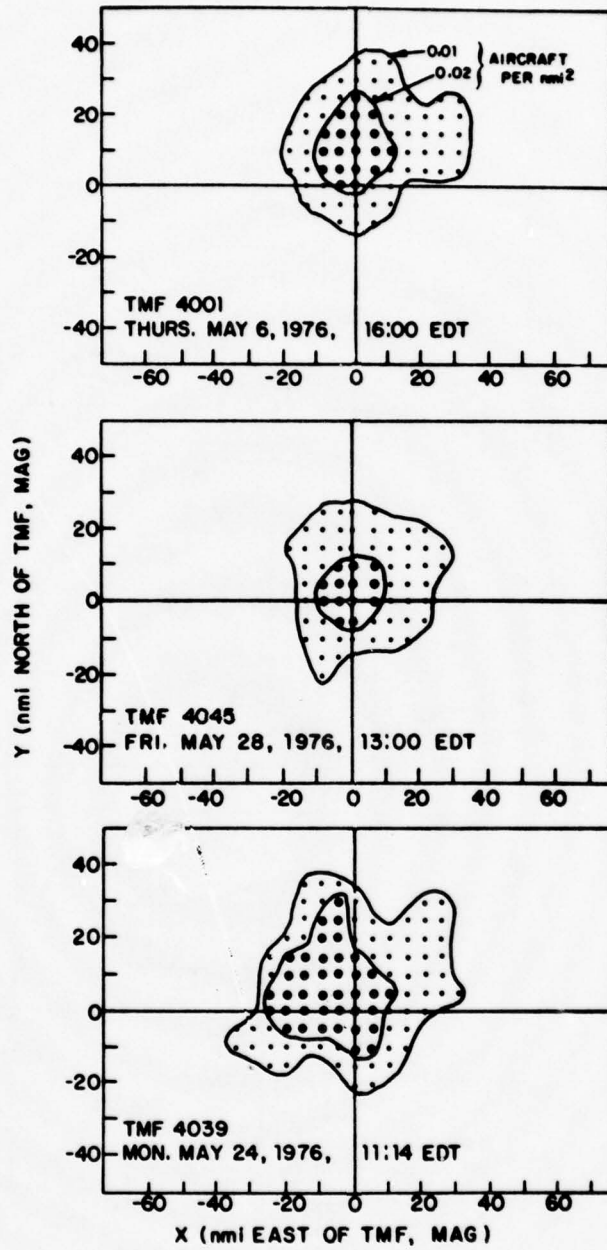


Fig.12. Day-to-day comparison of Washington traffic

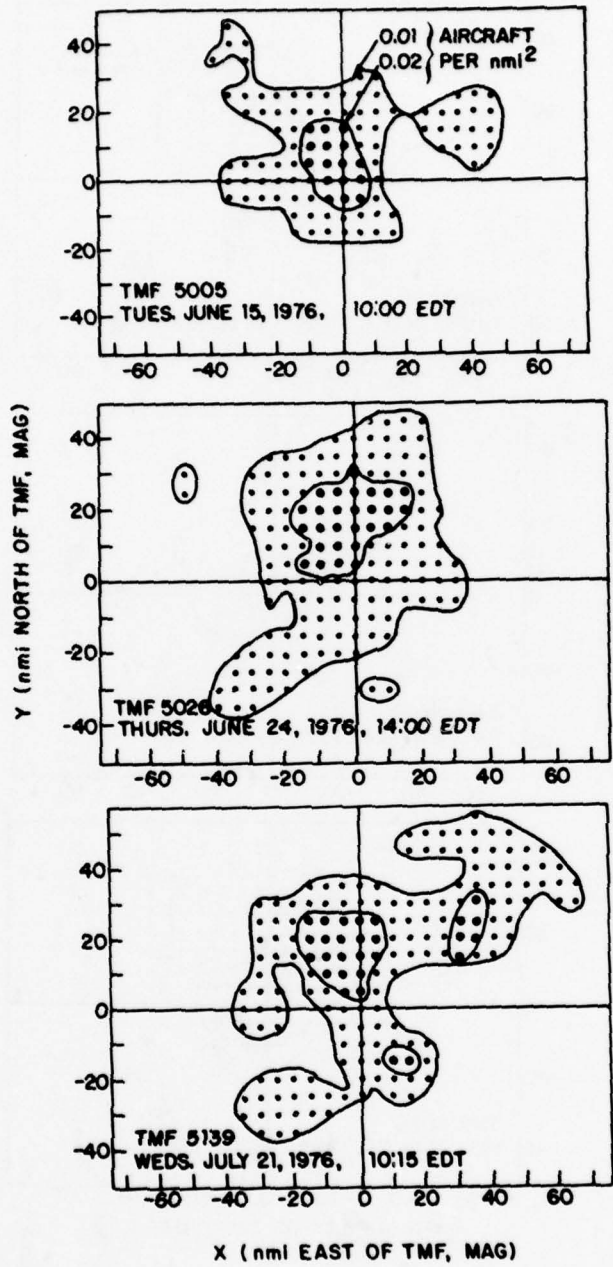


Fig.13. Day-to-day comparison of Philadelphia traffic

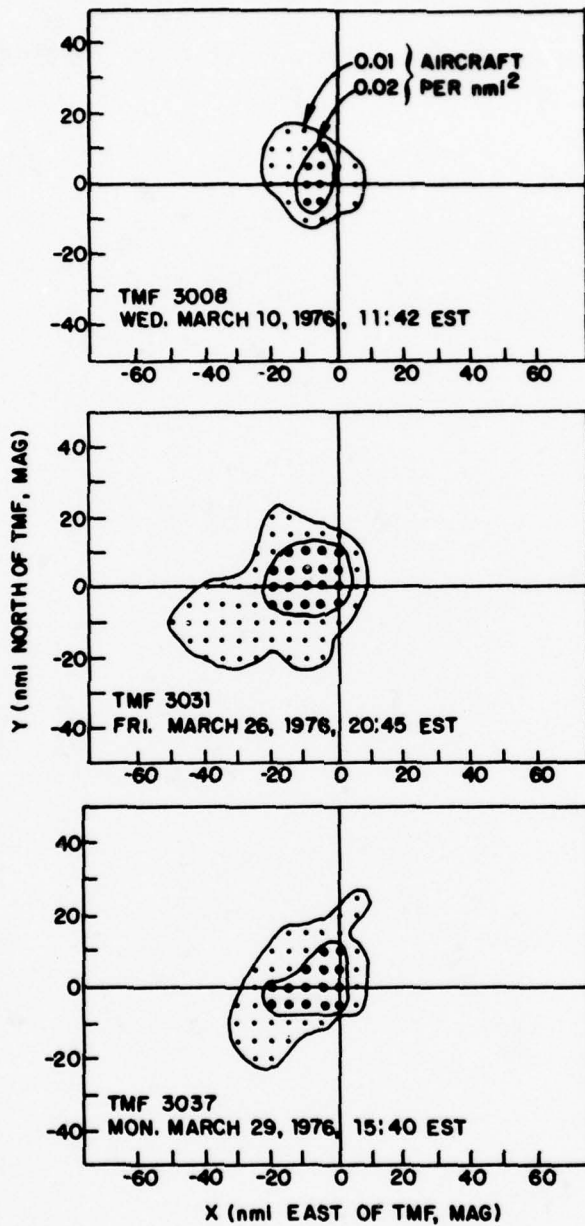


Fig.14. Day-to-day comparison of Boston traffic

fact that the Philadelphia traffic is much more uniformly distributed (as seen in Fig. 9), and so minor fluctuations in density can cause noticeable changes in the shapes of the shaded regions in Fig. 13.

More detailed computer outputs for all of these cases are given in the Appendix.

4.0 COMPARISON WITH THE STANDARD LA HIGH DENSITY MODEL

The LA Basin measurements have been compared with the LA Basin Standard Traffic Model (the high density 1982 model, ref. 6), herein called the "LA1" traffic model. A copy of the model was obtained on magnetic tape, and applied as the input to the traffic density analysis program. It was observed that traffic density increased steadily throughout the time period during which the model was taped, and for this reason the latter portion was selected for density analysis (time = 45856 to 46796 sec). The resulting density map (for R = 10 nmi) is shown in Fig. 15. Peak density, at $\rho = 0.48$ aircraft per sq. nmi, occurs in the Long Beach area, and about this location are computed the range histogram plotted in Fig. 16, the cumulative range distribution plotted in Fig. 11, and the instantaneous count of aircraft within 10 nmi plotted in Fig. 17. A straightforward comparison between model and measurement is shown in Fig. 18, where rotation and offset have been applied to adjust for the difference in origins and the difference between true and magnetic north. It is apparent that the model and the measurement agree closely in spatial distribution but differ in scale by about 5:1.

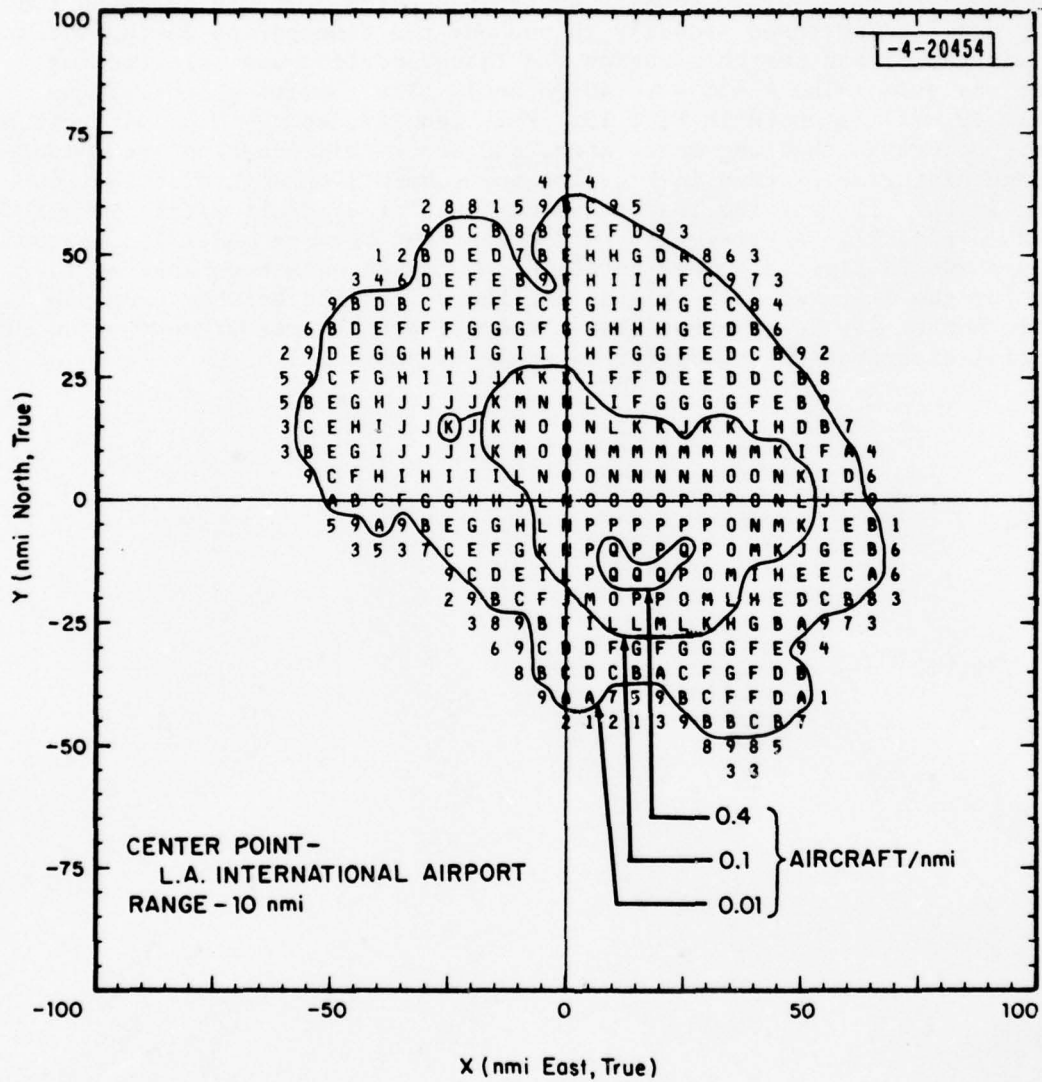


Fig.15. Traffic density map, LAI traffic model

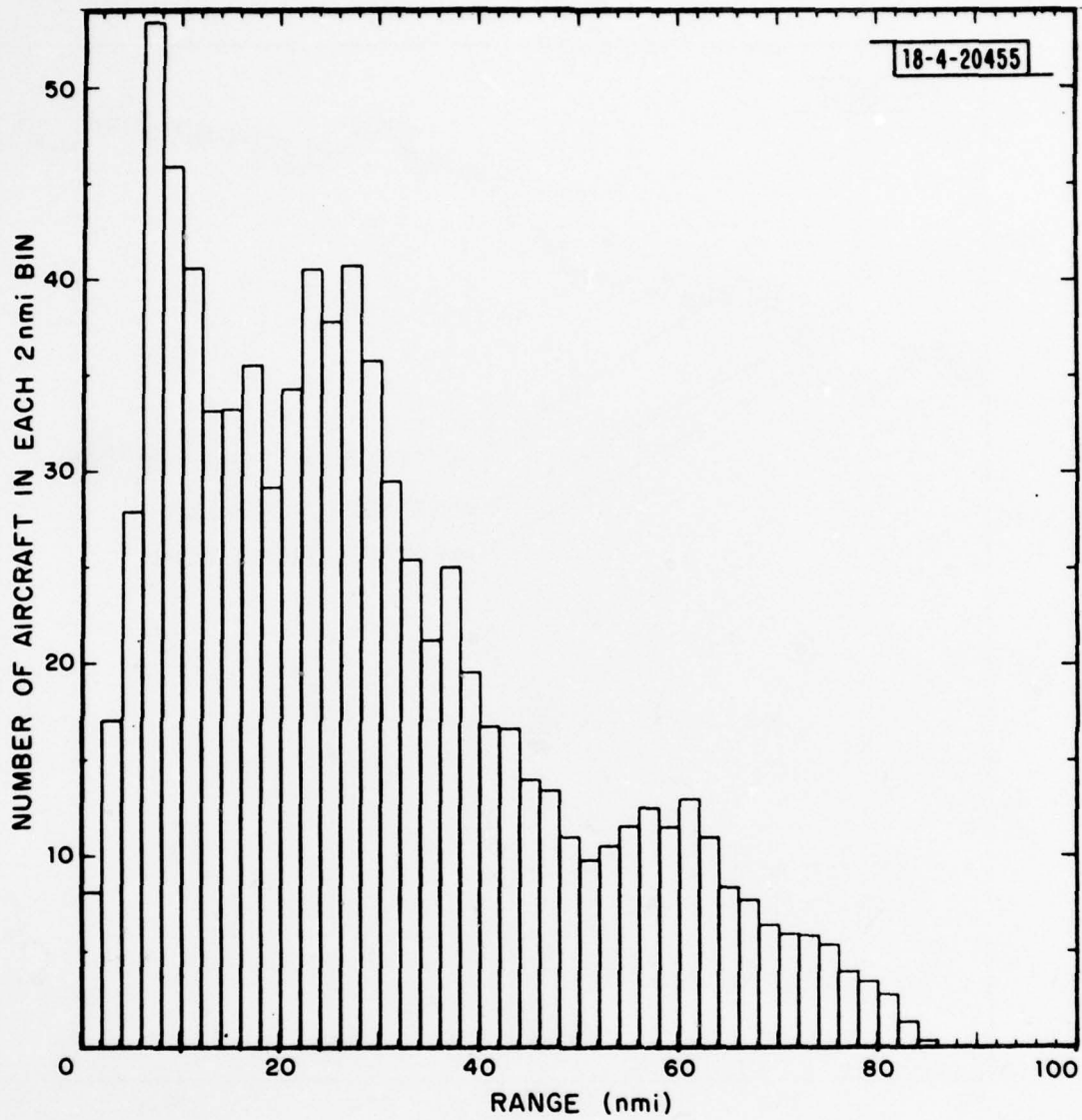


Fig.16. Range distribution histogram for the LA1 traffic model

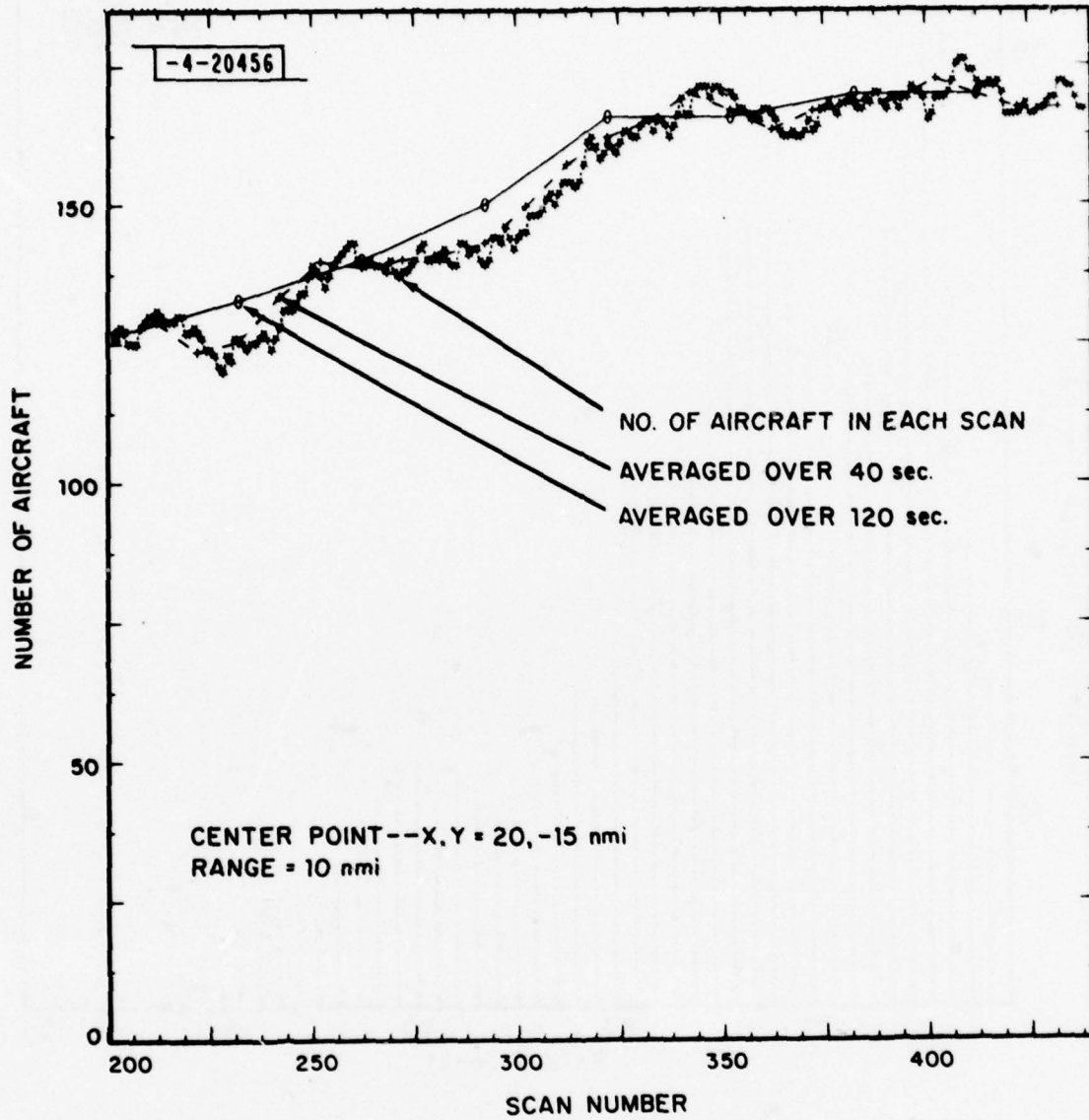


Fig.17. Time variation, LAL traffic model

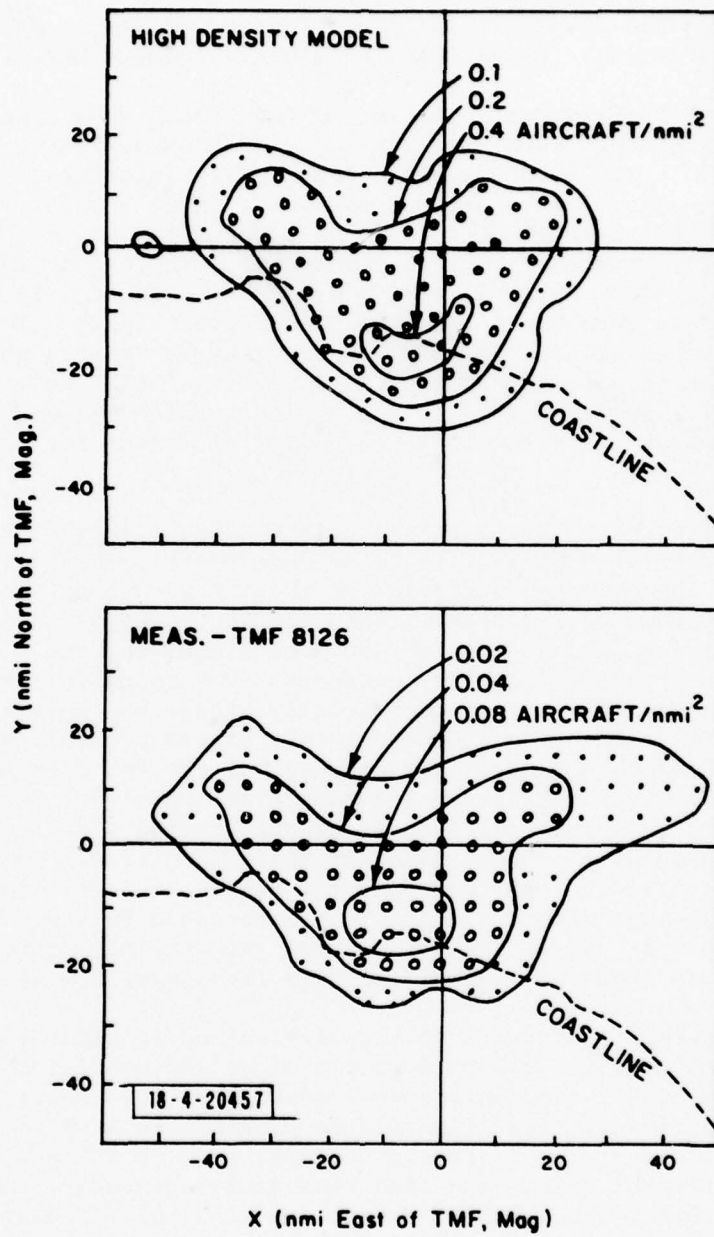


Fig.18. Comparison between LAI traffic model and TMF measurement

5.0 DATA VALIDITY

During the course of data reduction efforts a number of checks for validity of the results were made. Several of these are discussed here.

When the high traffic densities in the Long Beach area data were first observed a question arose as to the quality of TMF surveillance data under such conditions. It was asked whether high-density interference effects such as synchronous garbles, phantoms, and fruit might be disturbing the ATCRBS-mode data to a degree where these high densities may not be accurately measureable. This issue was studied by means of X-Y plots of TMF data showing traffic in the high density area. The example shown in Fig. 19 includes the area from Long Beach through LA International Airport (LAX). This is a plot of the first 50 scans of tape TMF8126, showing target reports which correlate with tracks. Landing and takeoff traffic patterns at LAX, Long Beach, and other airports are clearly evident. The quality of the TMF surveillance data is seen to be good and is believed to be quite sufficient for the present purpose.

All radar sites have coverage limitations to some degree, and these obviously interfere with the ability to measure traffic densities in the affected areas. The coverage qualities of the TMF Brea site were investigated in some detail because of the special interest in the LA Basin due to its high traffic concentration, and because of the mountainous terrain which may be expected to cause irregular coverage patterns. One specific area of interest is in the San Fernando Valley, in the vicinity of the Van Nuys and Burbank airports. These airports are noted for large numbers of small aircraft. Radar sites near LAX do not have good coverage of the San Fernando Valley because of the intervening Santa Monica Mountains. However, the TMF Brea site appears to be well located in this respect, having a relatively unobstructed view (from the southeast) of both sides of these mountains. While the TMF was at Brea, flight tests were conducted to measure low altitude coverage at a number of airports including those in the San Fernando Valley. Results are summarized in Table 1. These results confirm the original expectation that Brea is a good site, with widespread coverage throughout the LA Basin.

This study attempts to focus on the airborne environment and thus be independent to the greatest extent possible of ground conditions, such as parameters of the sensor and the precise location of the sensor. If this independence is achieved, then it should be possible to compare traffic density data recorded by two different sensors, such as TMF and ARTS-III, with slightly different sites, and find reasonable agreement. ARTS vs. TMF comparisons were carried out in two cases, one with the TMF/Deer Island compared with the ARTS at Boston Logan Airport, and the other between TMF and ARTS both located at Washington National Airport. In both cases, simultaneous recordings were used as inputs to the traffic density analysis program. The results, shown as traffic density maps are given in Figs. 20 and 21. Spatial distributions and absolute densities compare favorably, with ARTS showing slightly less traffic in both cases. This minor difference is probably attributable to the improvement in track reliabilities of TMF data relative to ARTS (Ref. 4).

C42-1618

TAPE TMF 8126

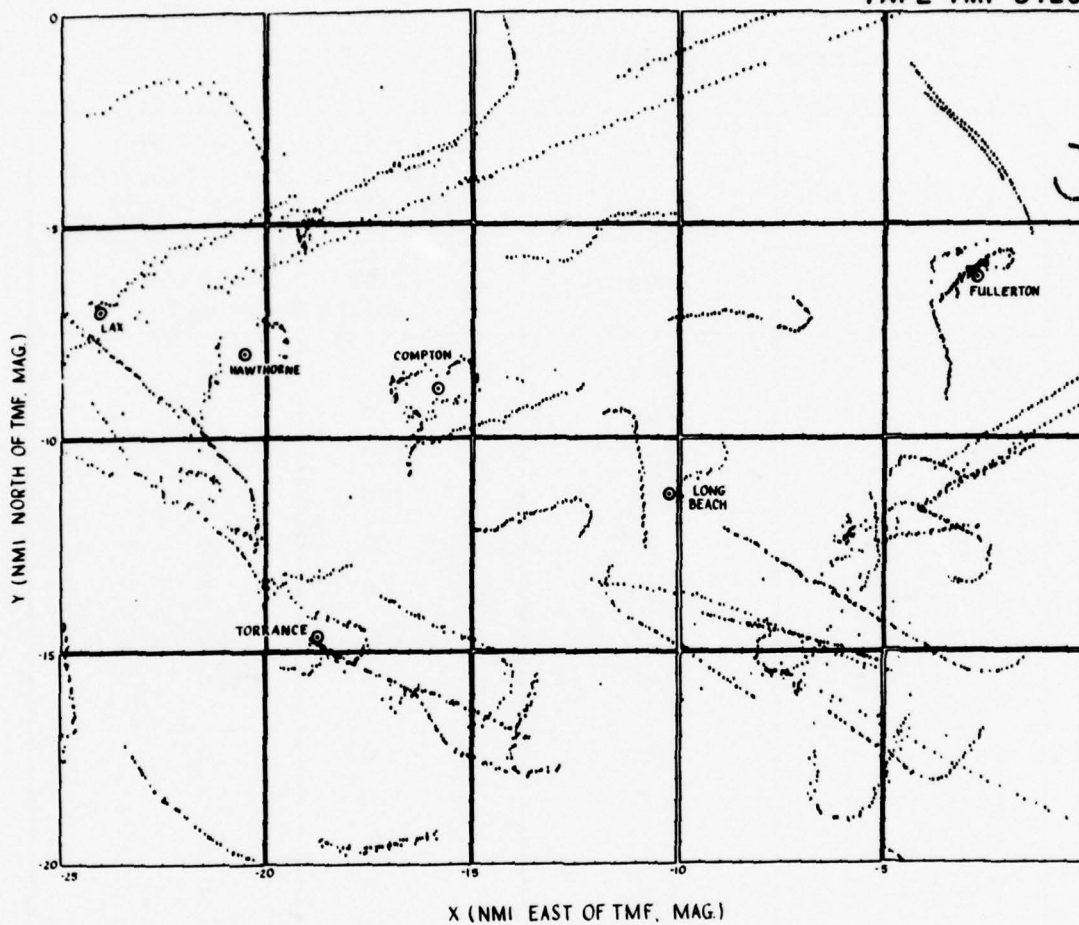


Fig.19. X-Y plot of aircraft tracks (LA Basin)

TABLE 1
MEASURED COVERAGE AT LA BASIN AIRPORTS

Airport	Airport Elevation (Ft. Above MSL)	Aircraft Altitude, Lower Limit of Surveillance Coverage (Ft. Above Ground Level)	
		During Landing	During Takeoff
Burbank	775	0	300
Brackett Field	1000	0	0
Chino	652	100	100
El Monte	296	0	0
Fullerton	96	0	0
Hawthorne	63	0	0
Long Beach	57	100	100
Los Angeles Intl.	126	0	100
Ontario	952	0	0
Orange County	54	0	0
Santa Monica	175	200	400
Torrance	101	0	0
Van Nuys	800	400	300

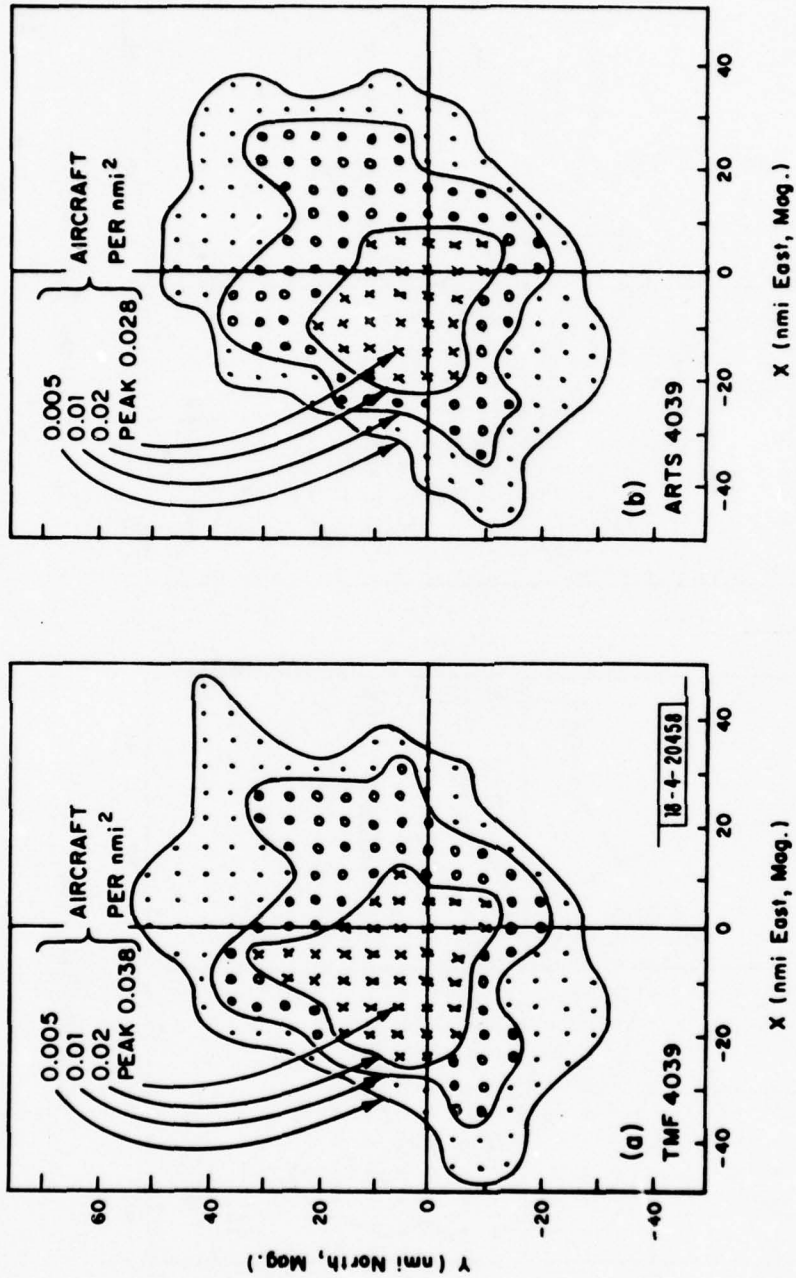


Fig.20. Comparison between TMF and ARTS as the source of traffic density data - Washington, D.C.

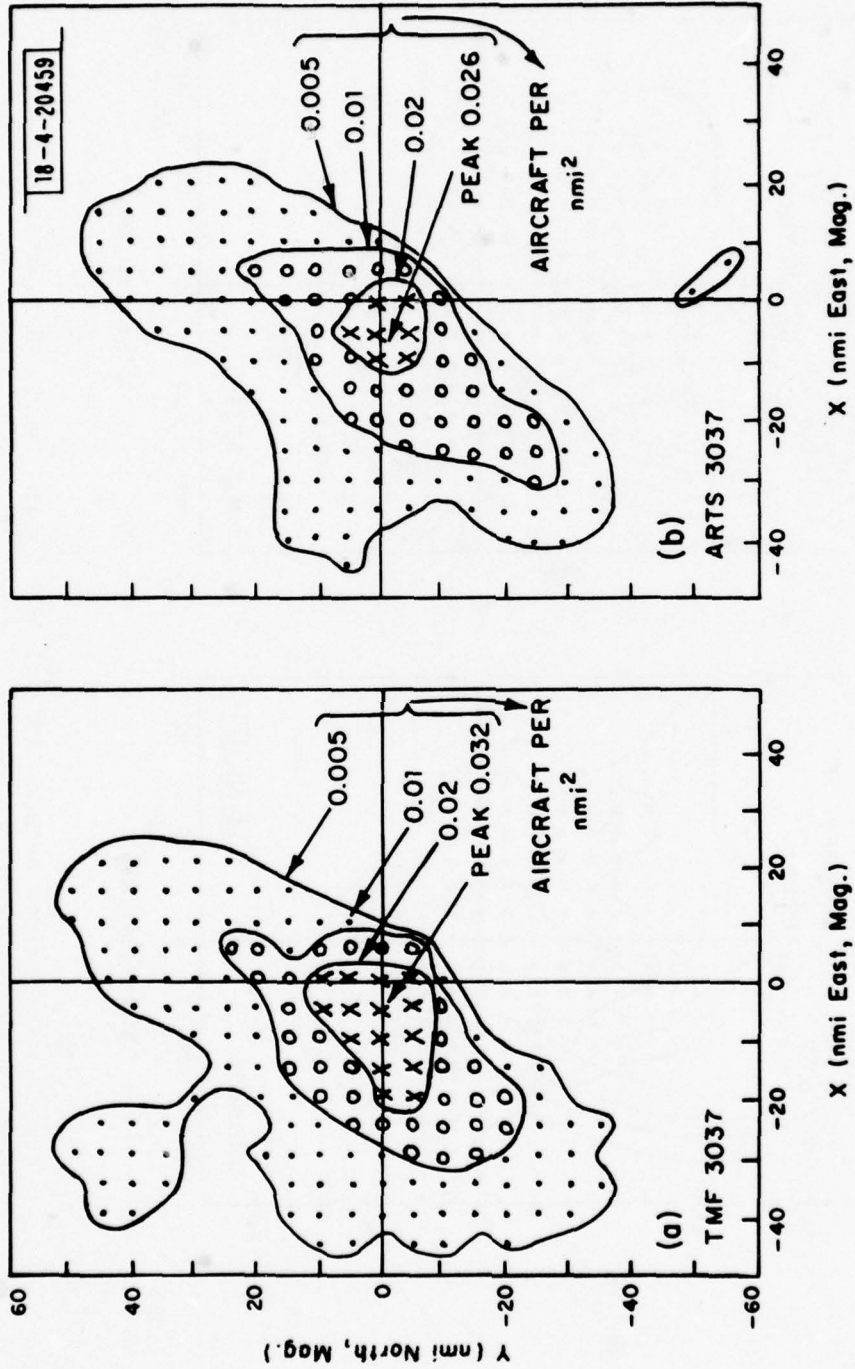


Fig.21. Comparison between TMF and ARTS as the source of traffic data - Boston

6.0 SUMMARY

Air traffic measurements in LA, Washington, Philadelphia, and Boston have shown that traffic density is the highest in LA. The time and spatial average density over a circular region of 10 nmi radius reaches a peak value of 0.1 aircraft/sq. nmi in LA. Under comparable conditions the densities in Washington, Philadelphia, and Boston reach 0.02 to 0.04 aircraft/sq. nmi. These measurements include only ATCRBS-transponder equipped aircraft.

These are peak densities which do not extend over large areas. Examination of the range distribution of aircraft relative to the point of highest density indicates that the region of constant density extends to a radius of about 10 to 15 nmi. Beyond that, the range distribution is better described as uniform-in-range, with a coefficient of about 3 aircraft/nmi in the case of LA.

These measurements, made in 1976, were compared with the LA1 Standard Traffic Model as to spatial distribution of traffic and absolute density. The results show that the model and the measurement differ by a scale factor of 5:1 (with density being greater in the model) but otherwise agree closely in spatial distribution.

REFERENCES

1. P.R. Drouilhet, "DABS: A System Description", Project Report ATC-42, Lincoln Laboratory, MIT, FAA-RD-74-189 (18 November 1974).
2. V.A. Orlando, J.D. Welch, "Beacon CAS (BCAS), An Integrated Air/Ground Collision Avoidance System", Project Report ATC-62, Lincoln Laboratory, MIT, FAA-RD-76-2 (23 March 1976).
3. W.H. Harman, et al, "Discrete Address Beacon System (DABS) Test Plan for FY1976", Project Report ATC-56, Lincoln Laboratory, MIT, FAA-RD-75-145, (14 November 1975), p. 7-10.
4. W.I. Wells, "Verification of DABS Sensor Surveillance Performance (ATCRBS-mode) at Typical ASR Sites Throughout CONUS", Project Report ATC-79, Lincoln Laboratory, MIT FAA-RD-77-113 (20 December 1977).
5. "Reference Data for Radio Engineers", ITT, Fifth Edition (1968) pp. 39-5.
6. "User's Manual for the Los Angeles Basin Standard Traffic Model", MITRE Corp., FAA-RD-73-88, p. 73.

APPENDIX
DETAILED COMPUTER OUTPUTS

For each of the TMF measurements discussed in Sections 2 and 3, the traffic density map and the range distribution histogram, centered at the location of highest density, are given in this appendix. The traffic density maps all indicate density by the same log scale as defined in Fig. 1, and in all cases the density is the average within a radius of 10 nmi.

Table A1 serves as a listing of the contents of this Appendix and also includes the date and time-of-day of each measurement.

TABLE A1
CONTENTS OF THE APPENDIX

<u>Measurement No.</u>	<u>Location</u>	<u>-Figure No.- Map Histogram</u>	<u>Date of Measurement</u>	<u>Day</u>	<u>Local Time</u>	<u>Max. Time- and Spatial- Average Aircraft Count, R=10 nmi.</u>
TMF 8126	LA	A1 A2	21 Nov. 76	Sun.	11:30-11:49 PST	30
TMF 8122	LA	A3 A4	20 Nov. 76	Sat.	14:00-14:18 PST	26
TMF 8046	LA	A5 A6	11 Nov. 76	Thurs.	16:26-16:45 PST	26
TMF 8055	LA	A7 A8	15 Nov. 76	Mon.	12:38-12:56 PST	21
TMF 4039	Washington	A9 A10	24 May 76	Mon.	11:14-11:34 EDT	12
TMF 4001	Washington	A11 A12	6 May 76	Thurs.	15:57-16:21 EDT	8
TMF 4054	Washington	A13 A14	28 May 76	Fri.	12:58-13:24 EDT	8
TMF 5139	Phila.	A15 A16	21 July 76	Wed.	10:14-10:26 EDT	11
TMF 5026	Phila.	A17 A18	24 June 76	Thurs.	13:58-14:28 EDT	8
TMF 5005	Phila.	A19 A20	15 June 76	Tues.	09:55-10:08 EDT	9
TMF 3031	Boston	A21 A22	26 March 76	Fri.	20:45-21:04 EST	12
TMF 3037	Boston	A23 A24	29 March 76	Mon.	15:41-15:59 EST	10
TMF 3008	Boston	A25 A26	10 March 76	Wed.	11:42-12:12 EST	8

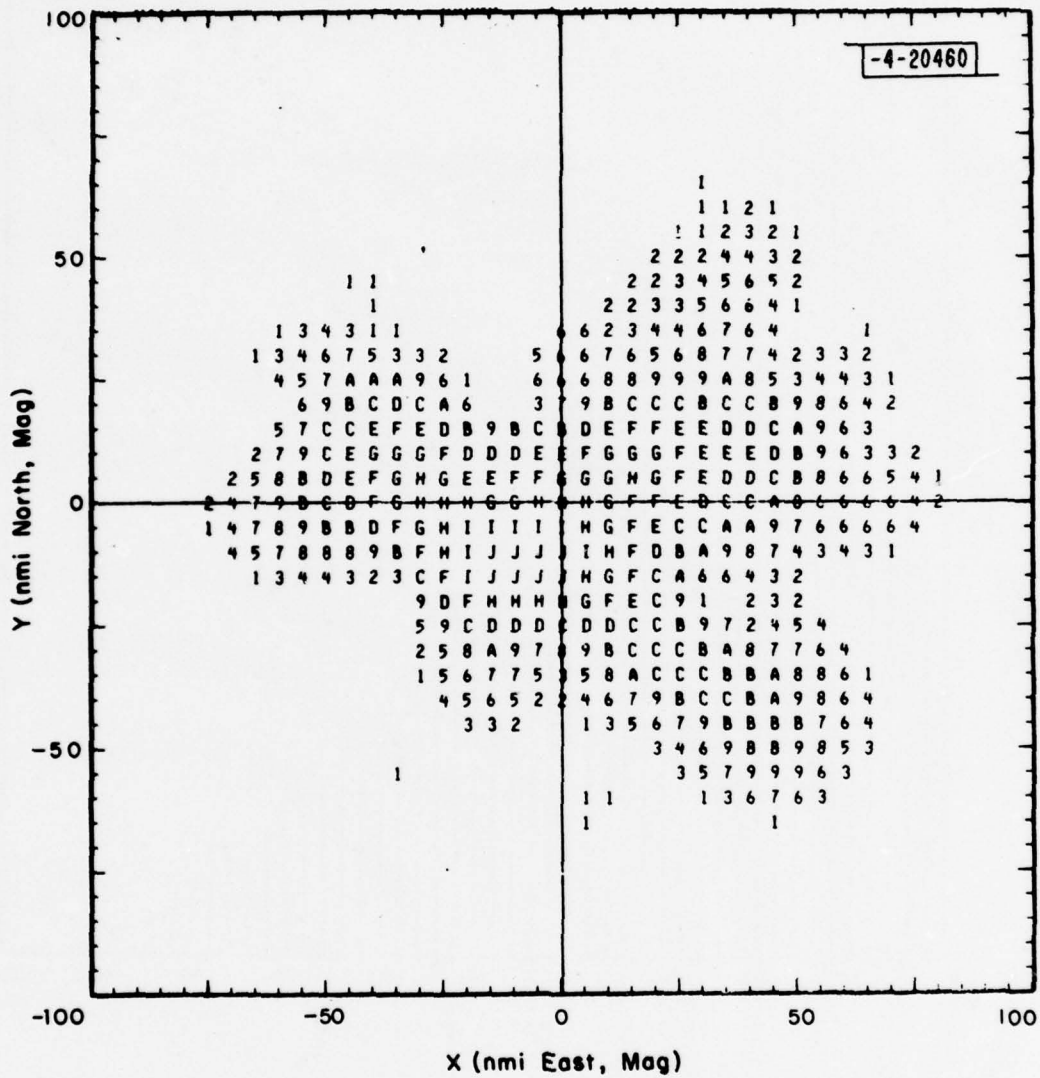


Fig.A-1. LA map, TMF8126

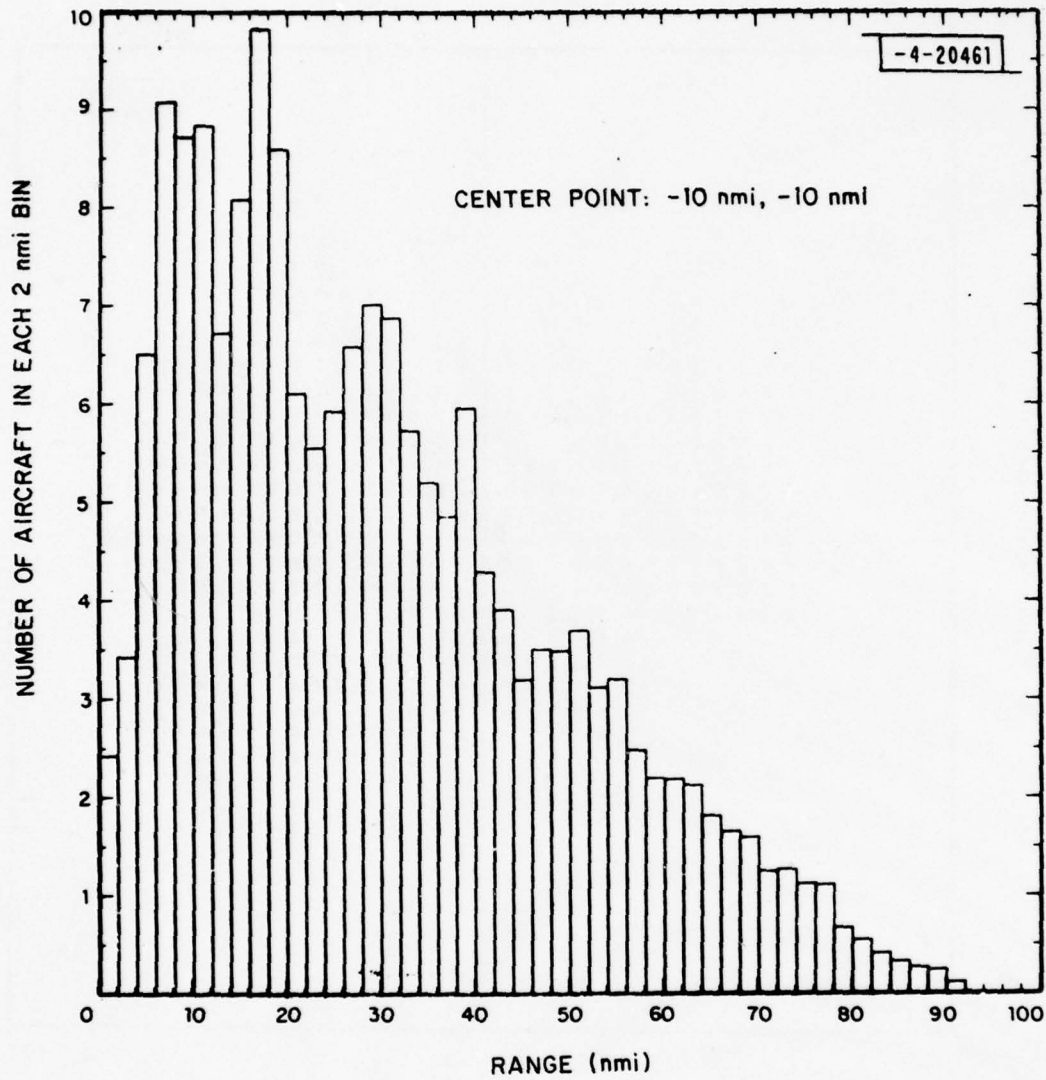


Fig.A-2. LA histogram, TMF8126

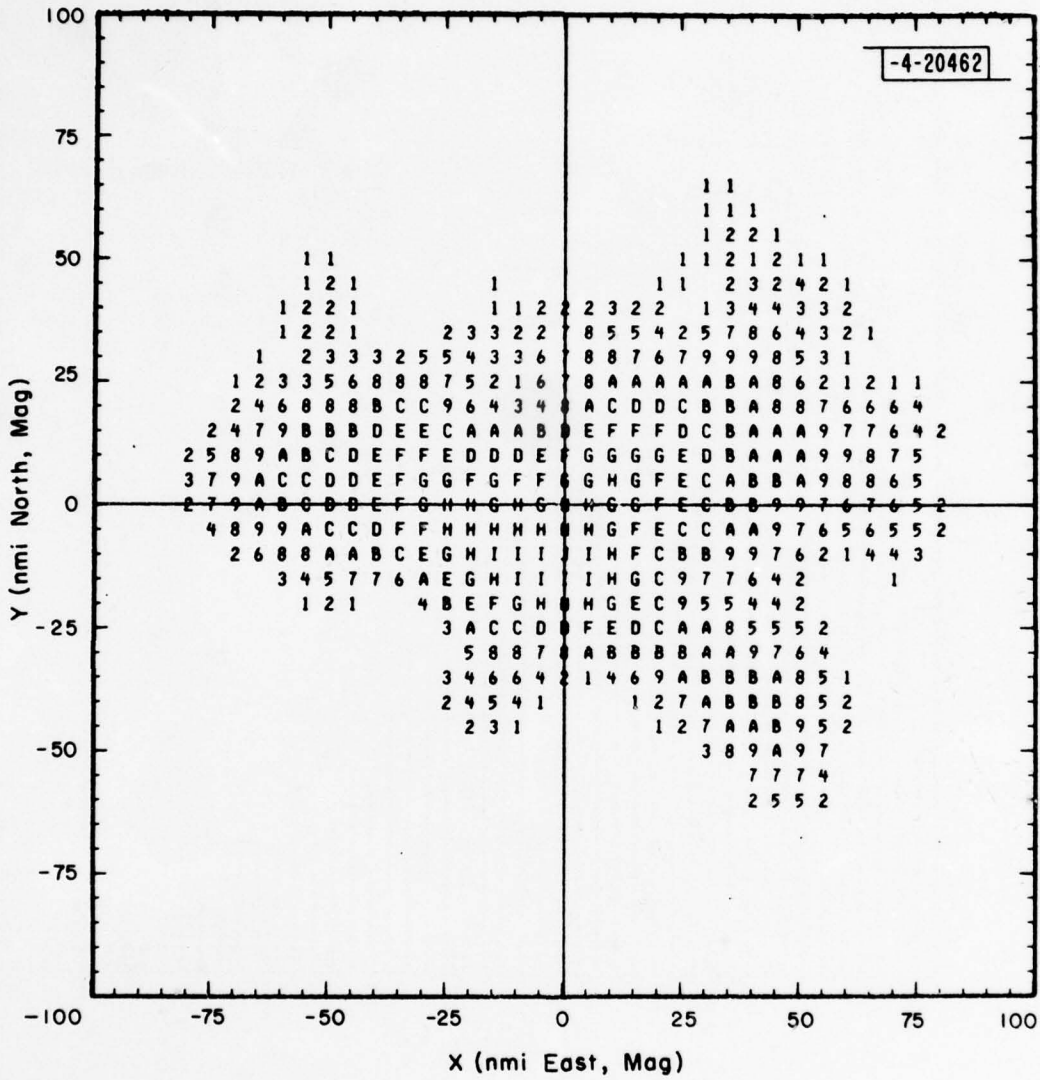


Fig.A-3. LA map, TMF8122

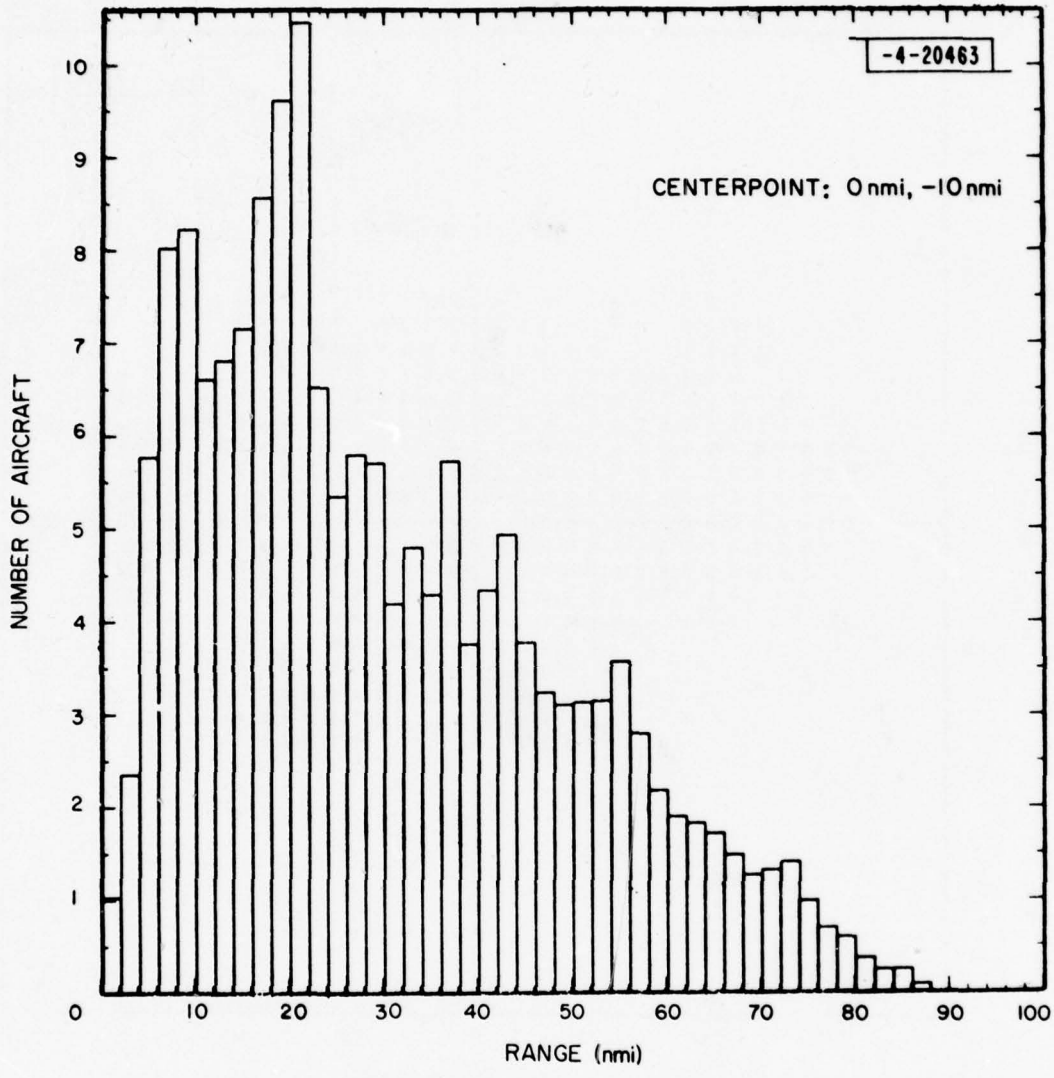


Fig.A-4. LA histogram, TMF8122

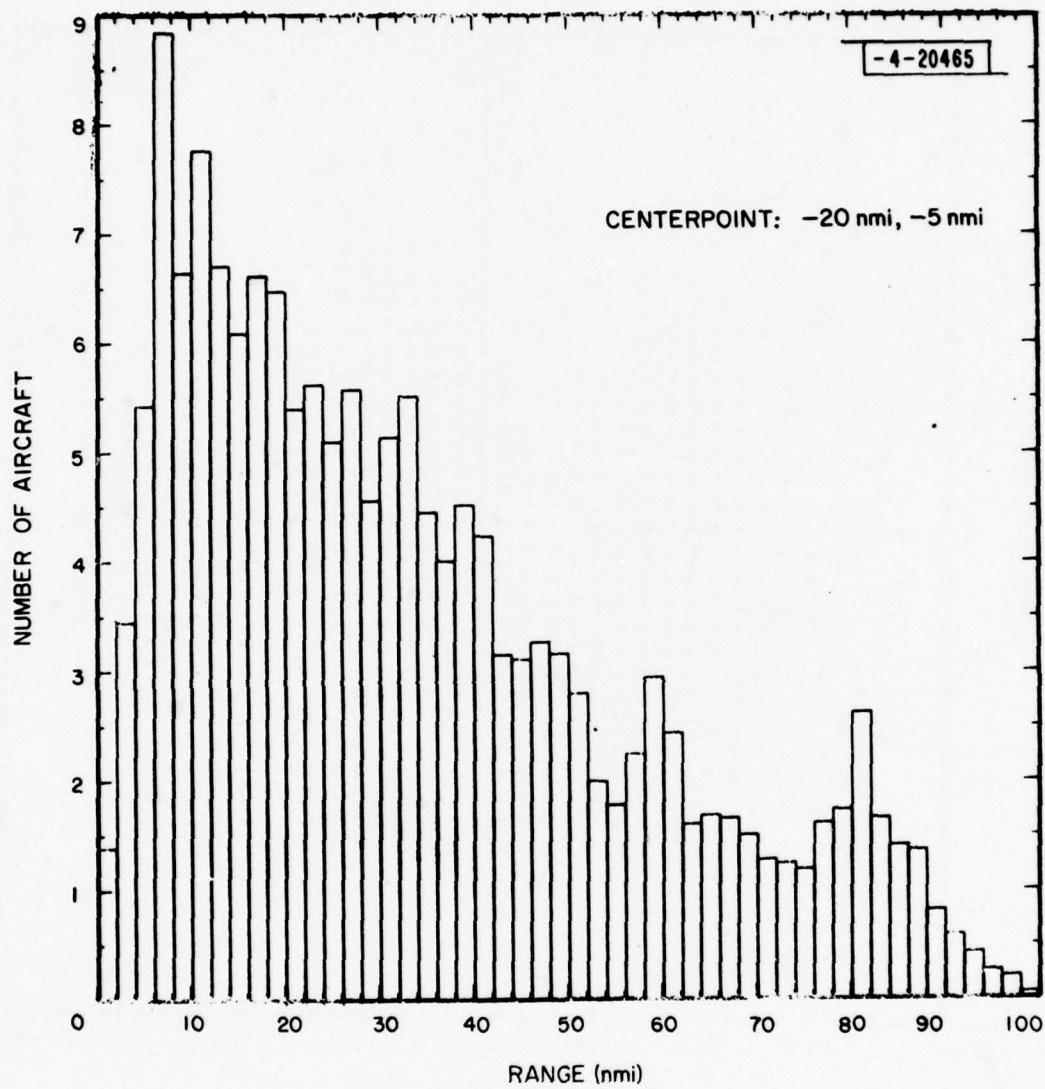
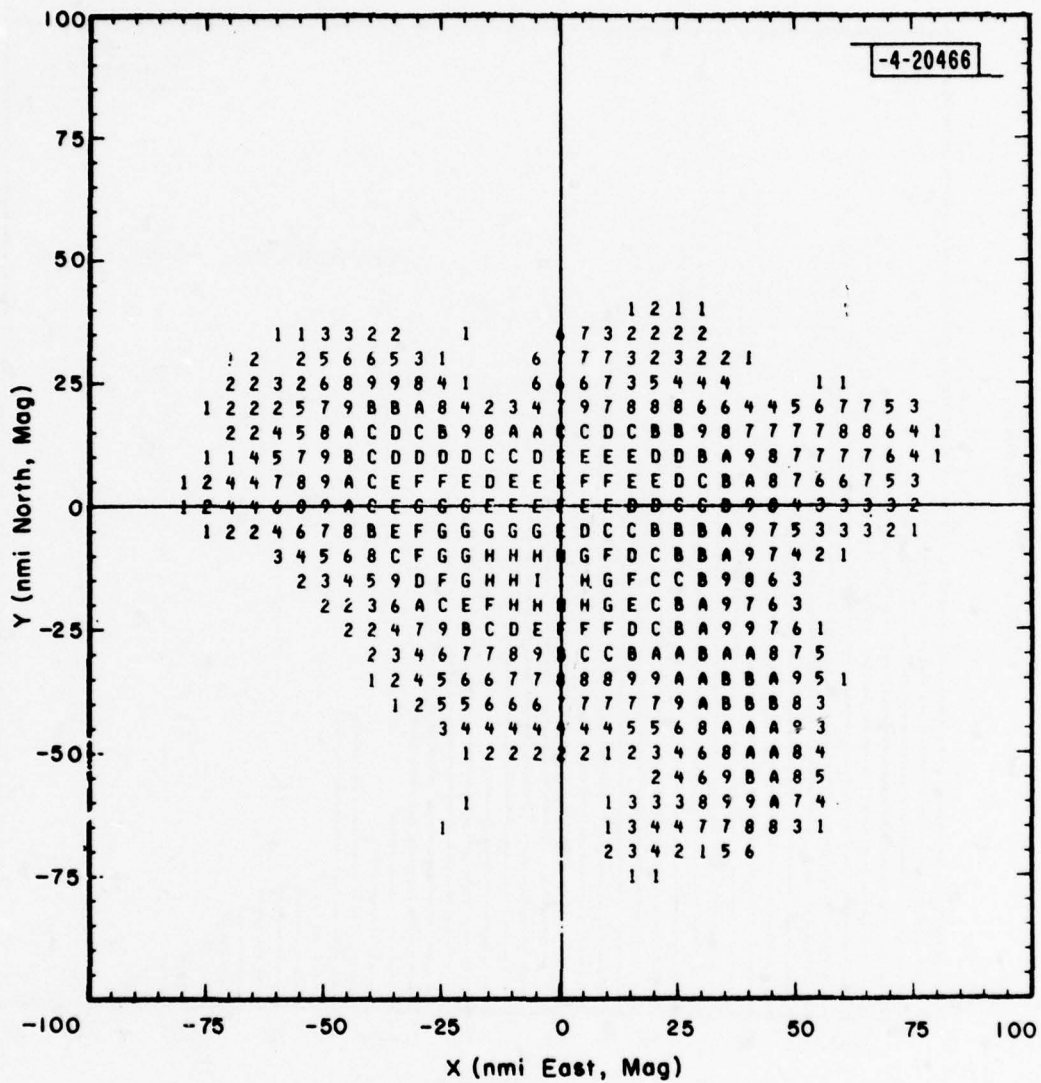


Fig.A-6. LA histogram, TMF8046



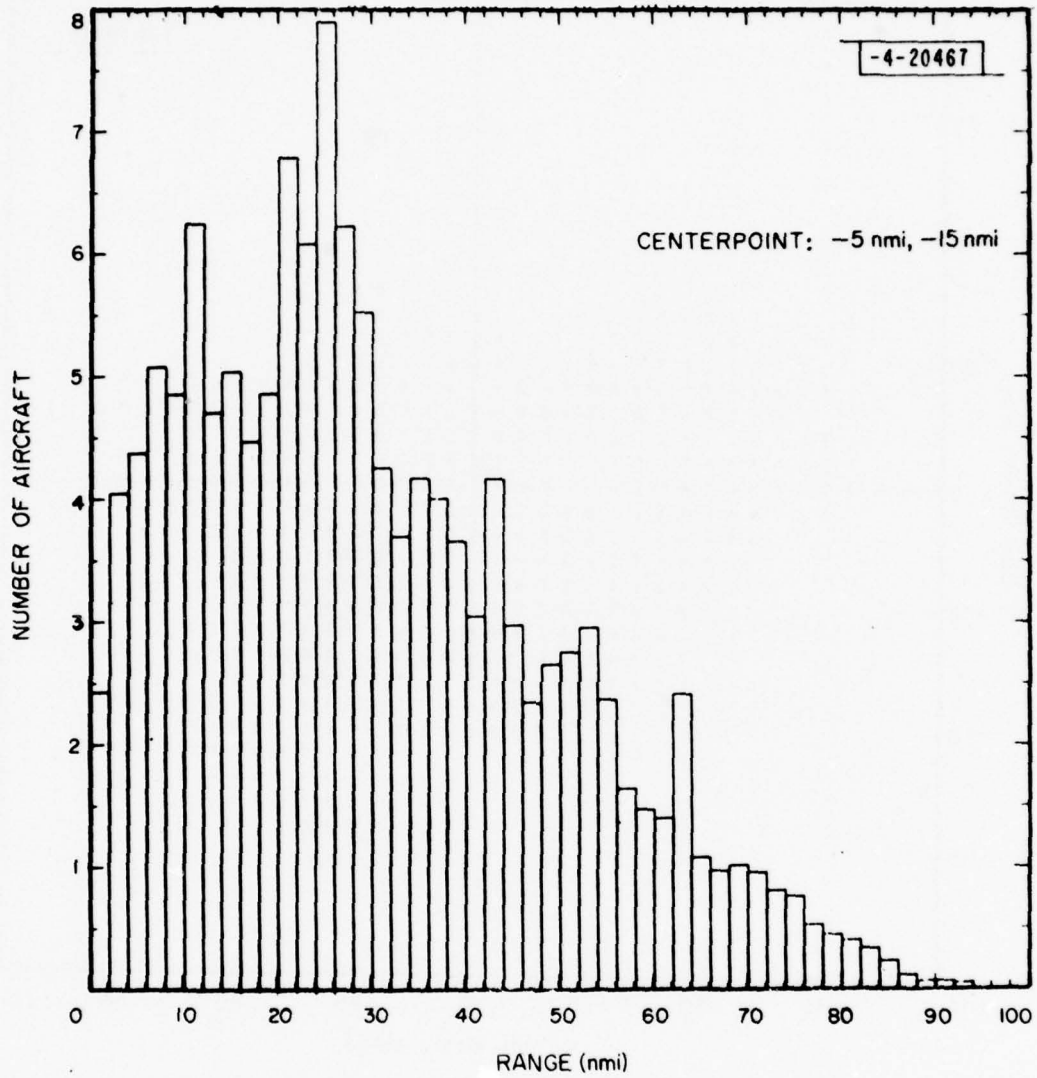


Fig. A-8. LA histogram, TMF8055

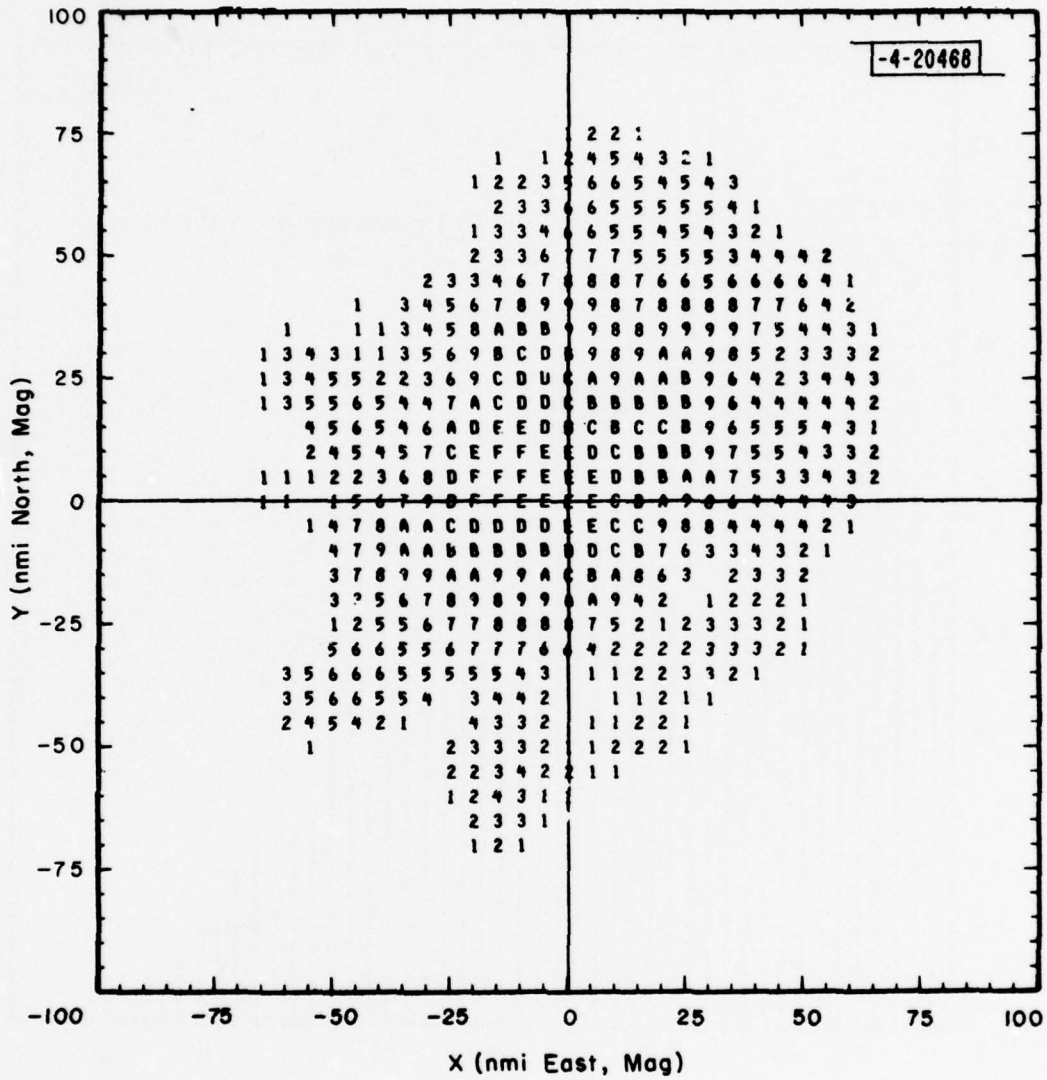


Fig.A-9. Washington map, TMF4039

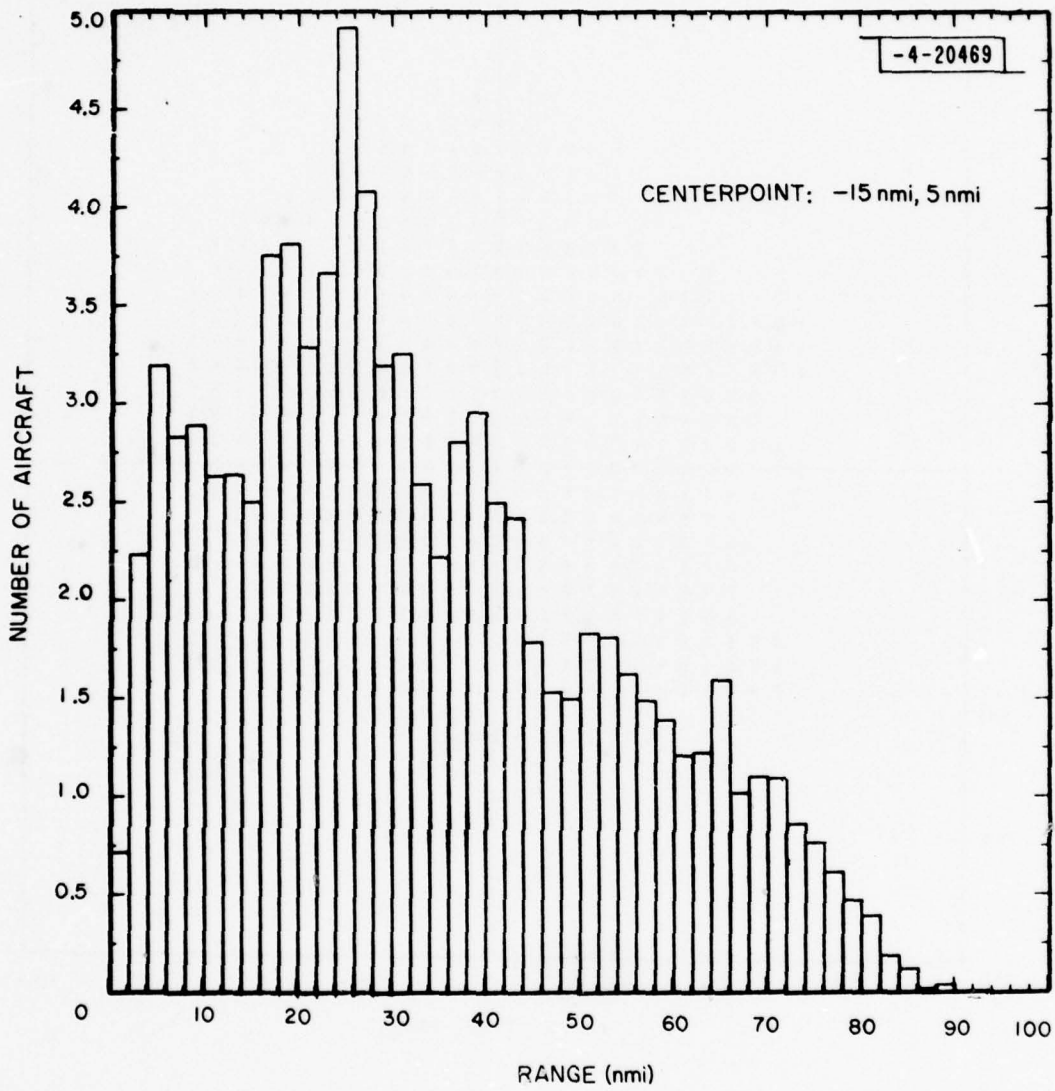


Fig.A-10. Washington histogram, TMF4039

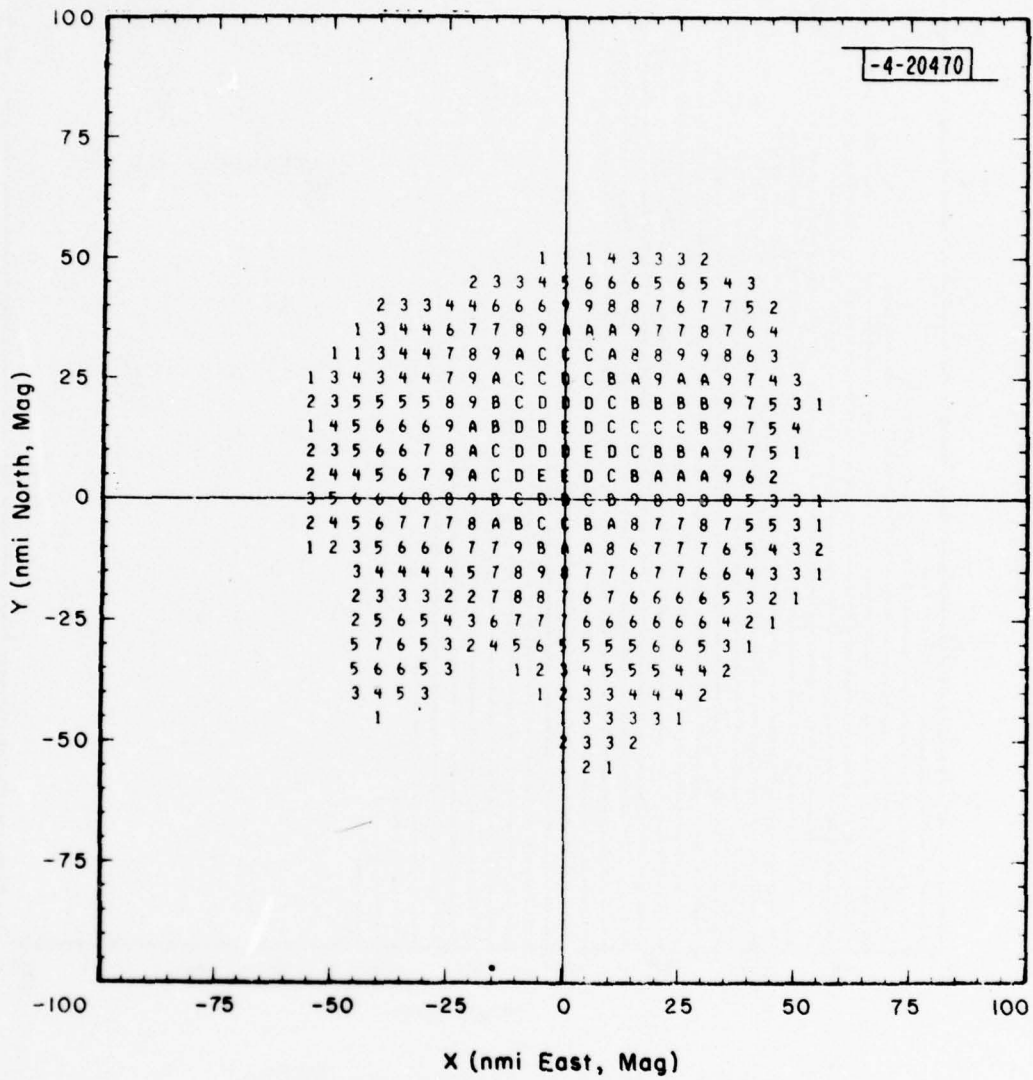


Fig.A-11. Washington map, TMF4001

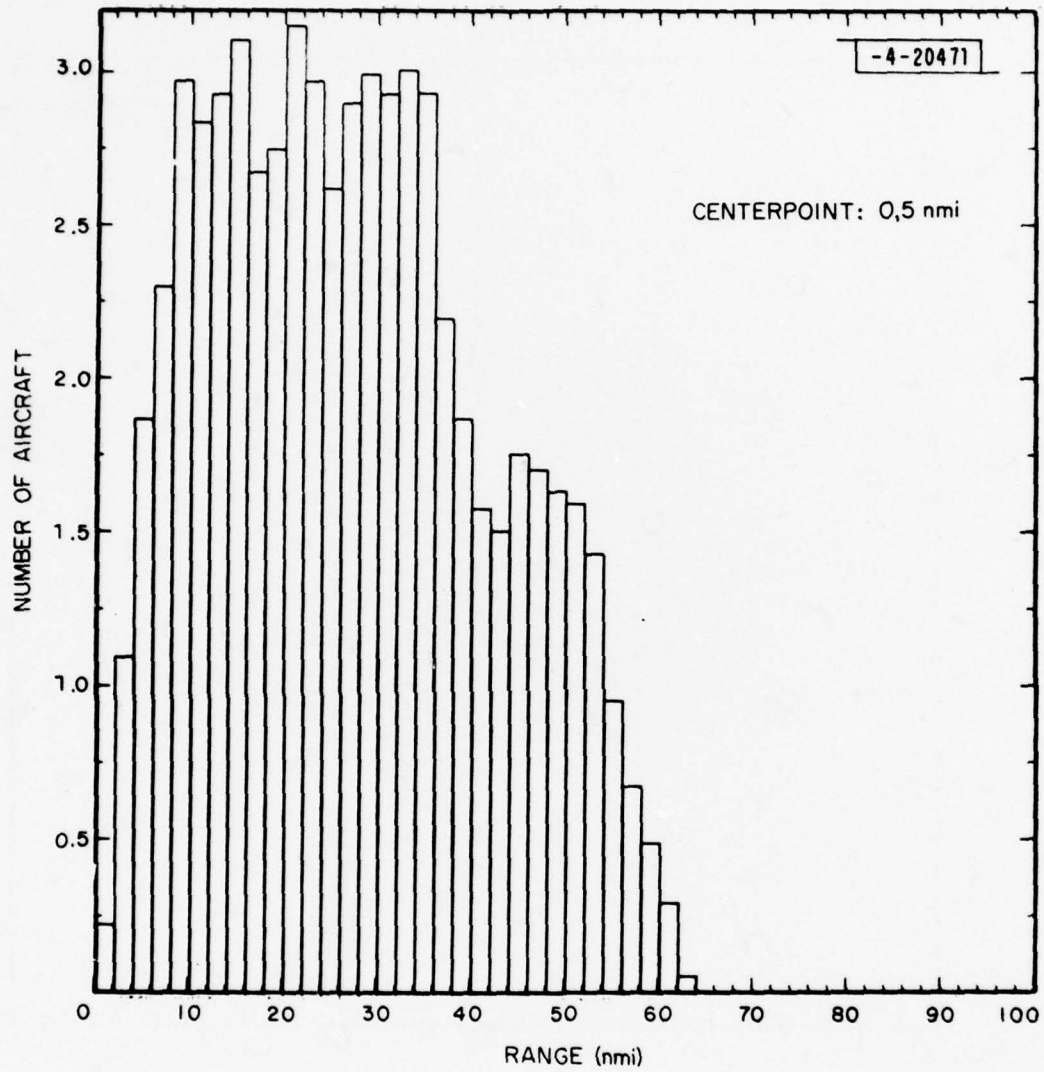


Fig.A-12. Washington histogram, TMF4001

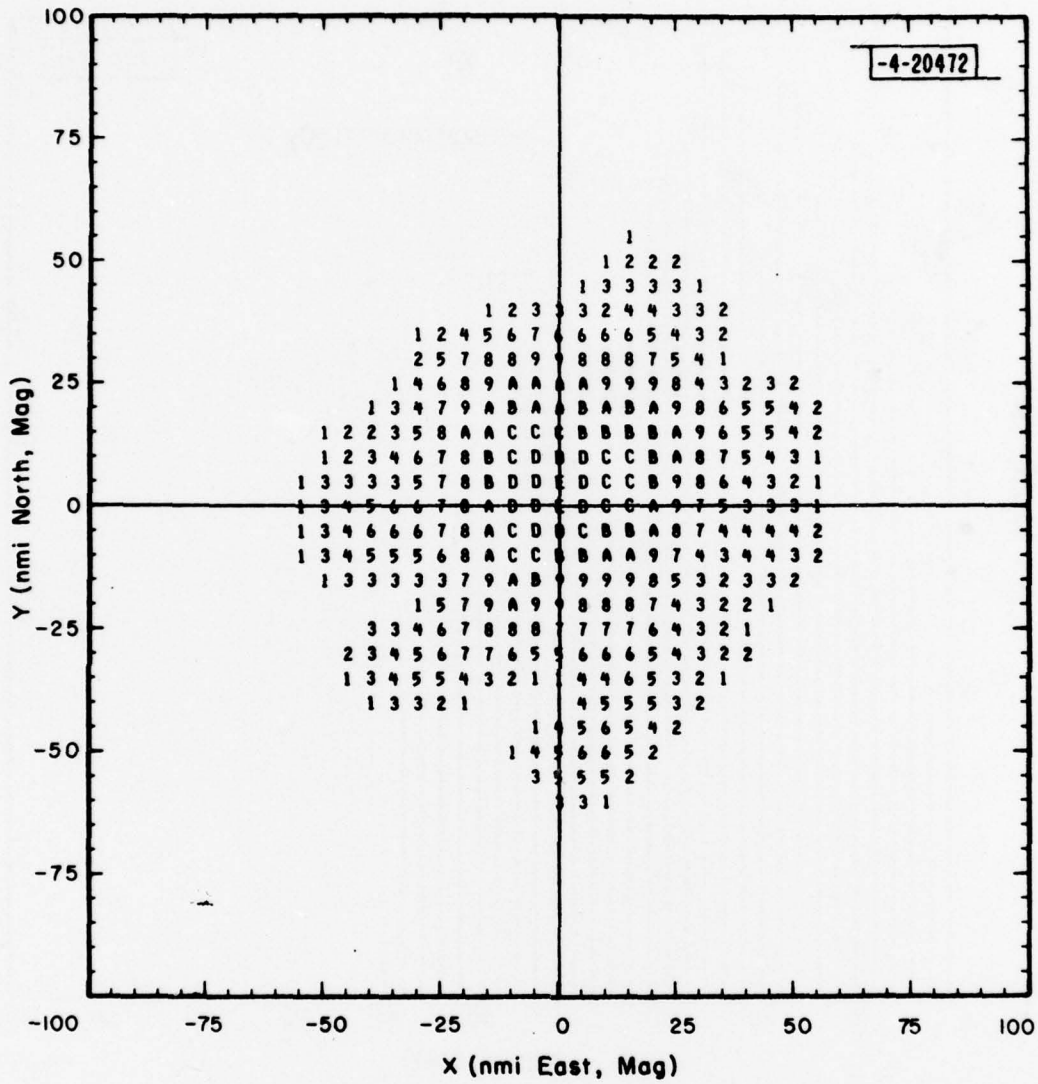


Fig.A-13. Washington map, TMF4054

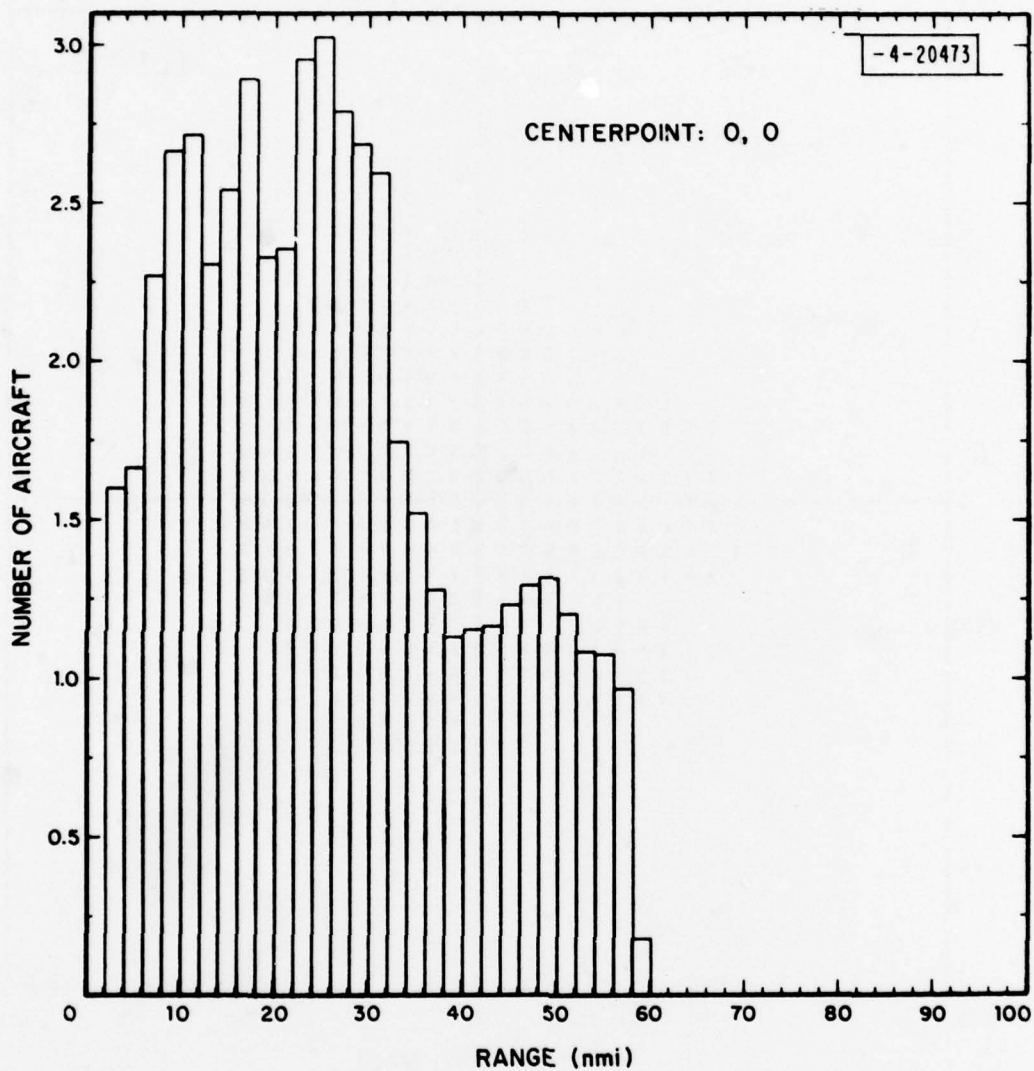


Fig.A-14. Washington histogram, TMF4054

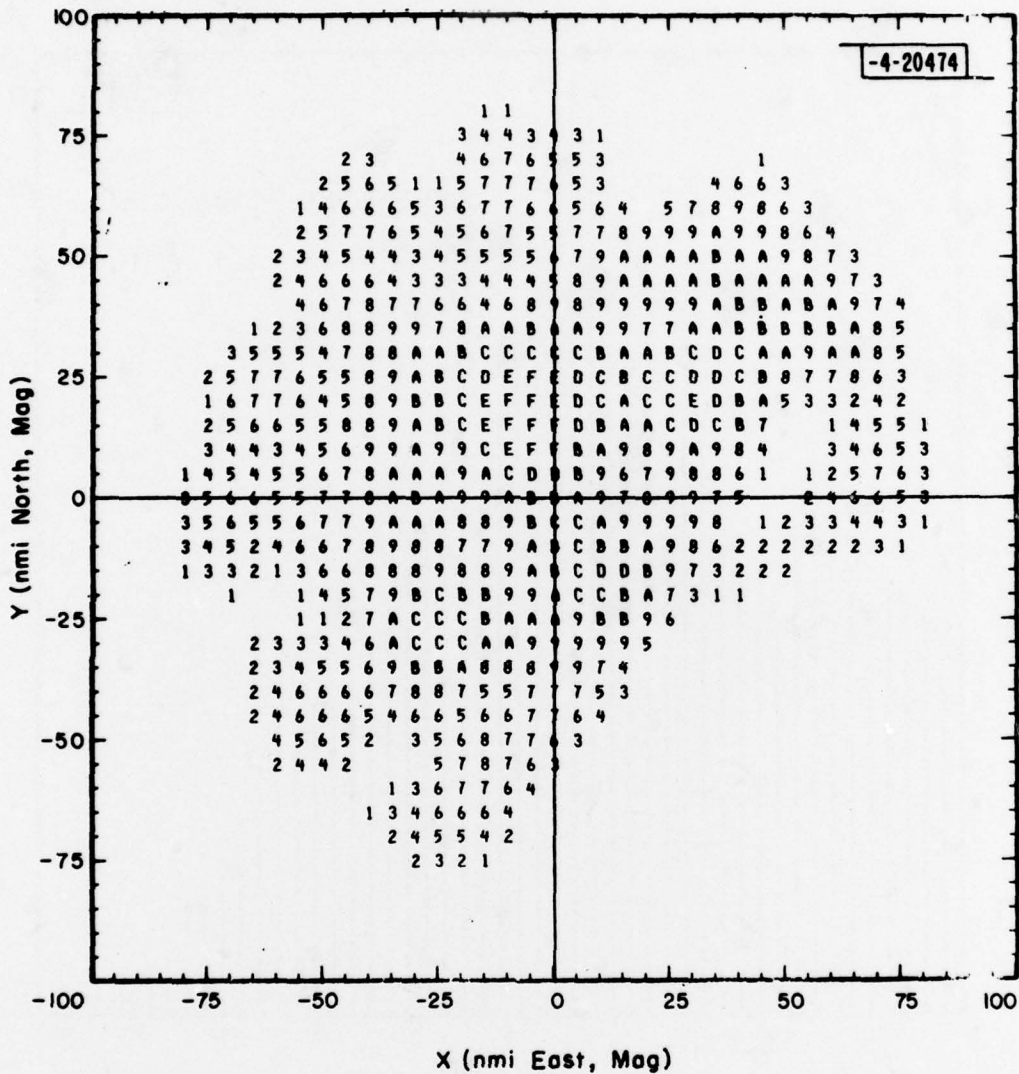


Fig.A-15. Philadelphia map, TMF5139

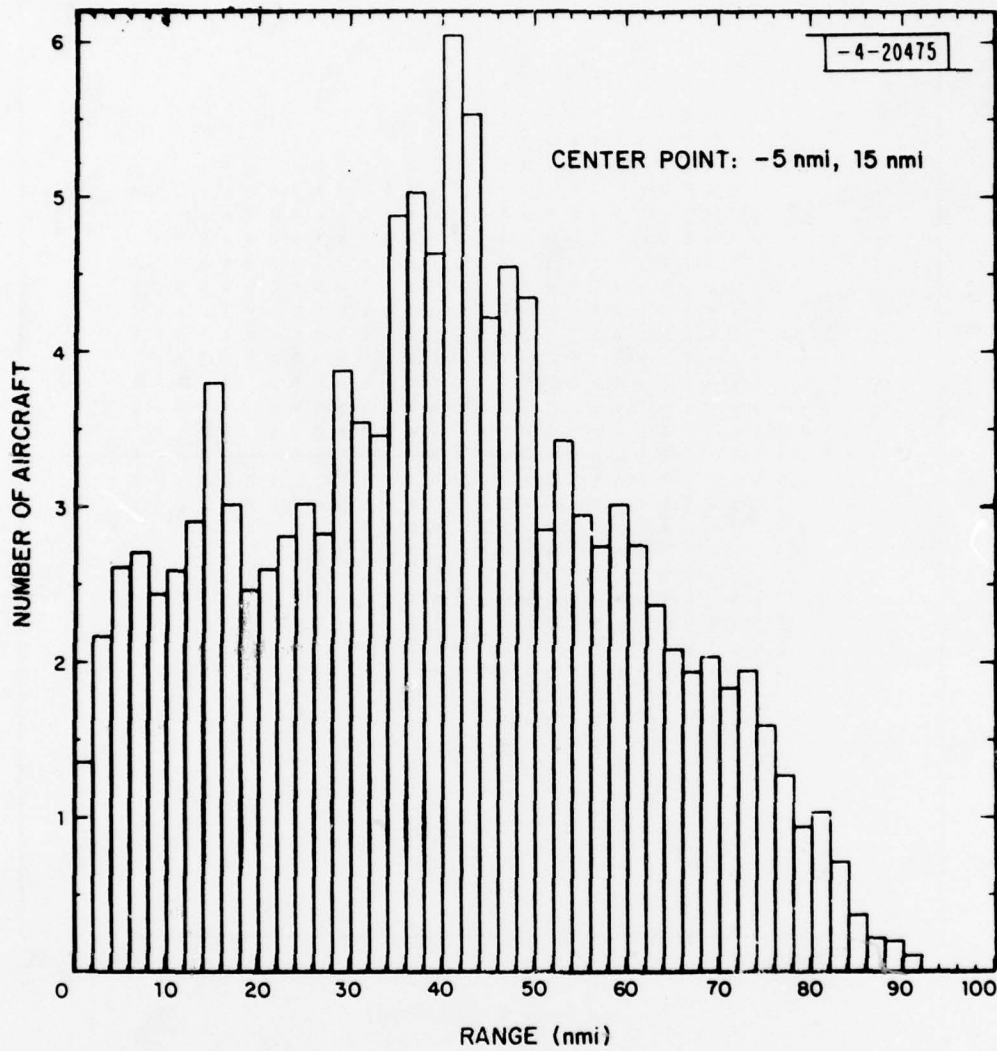


Fig.A-16. Philadelphia histogram, TMF5139

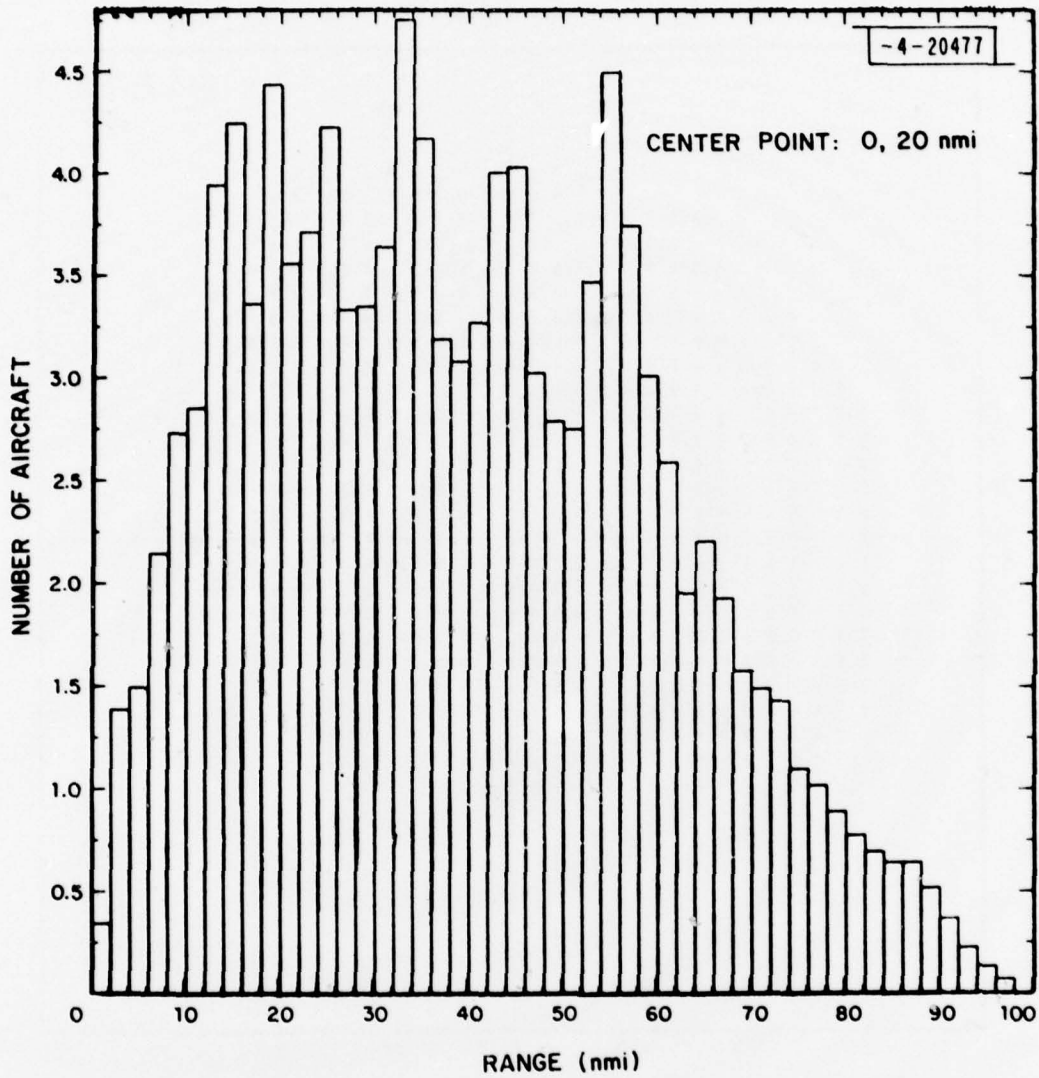


Fig.A-18. Philadelphia histogram, TMF5026

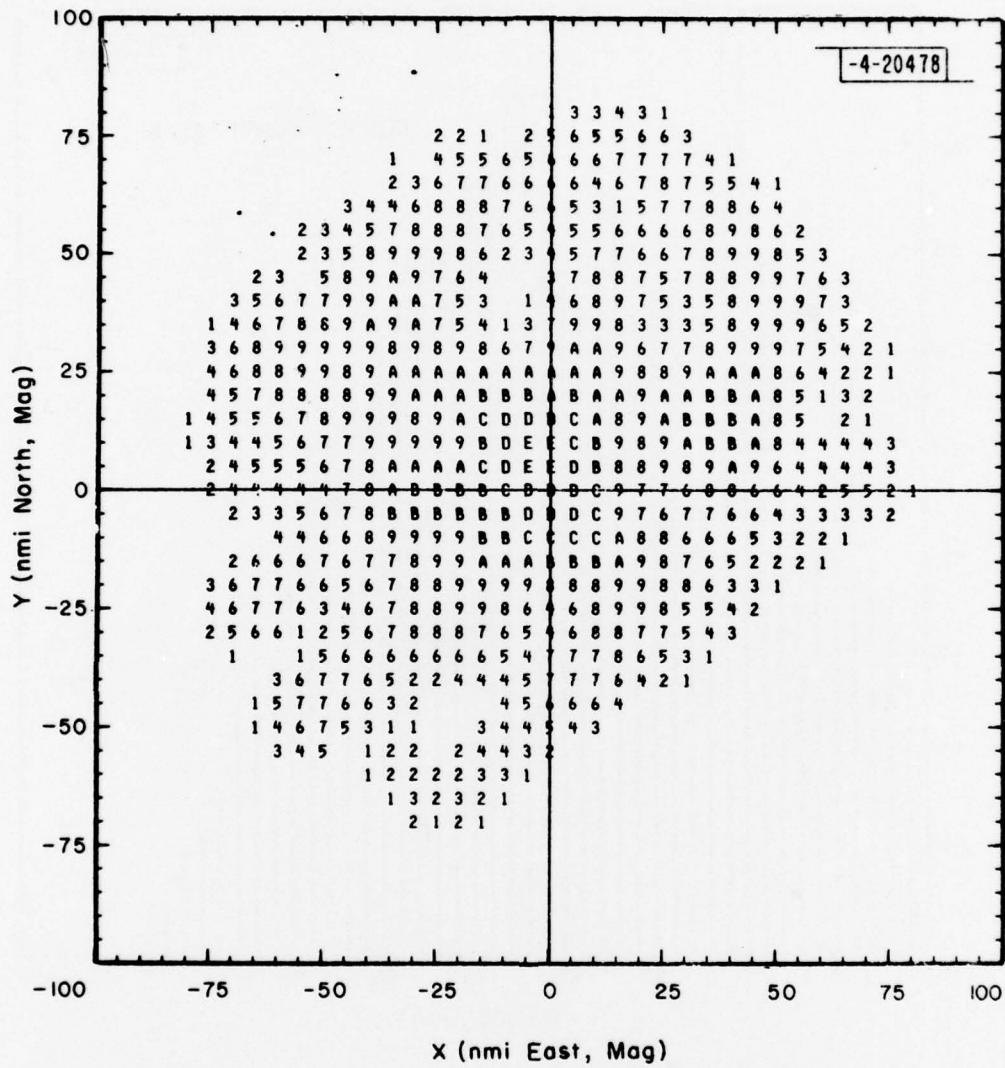


Fig.A-19. Philadelphia map, TMF5005

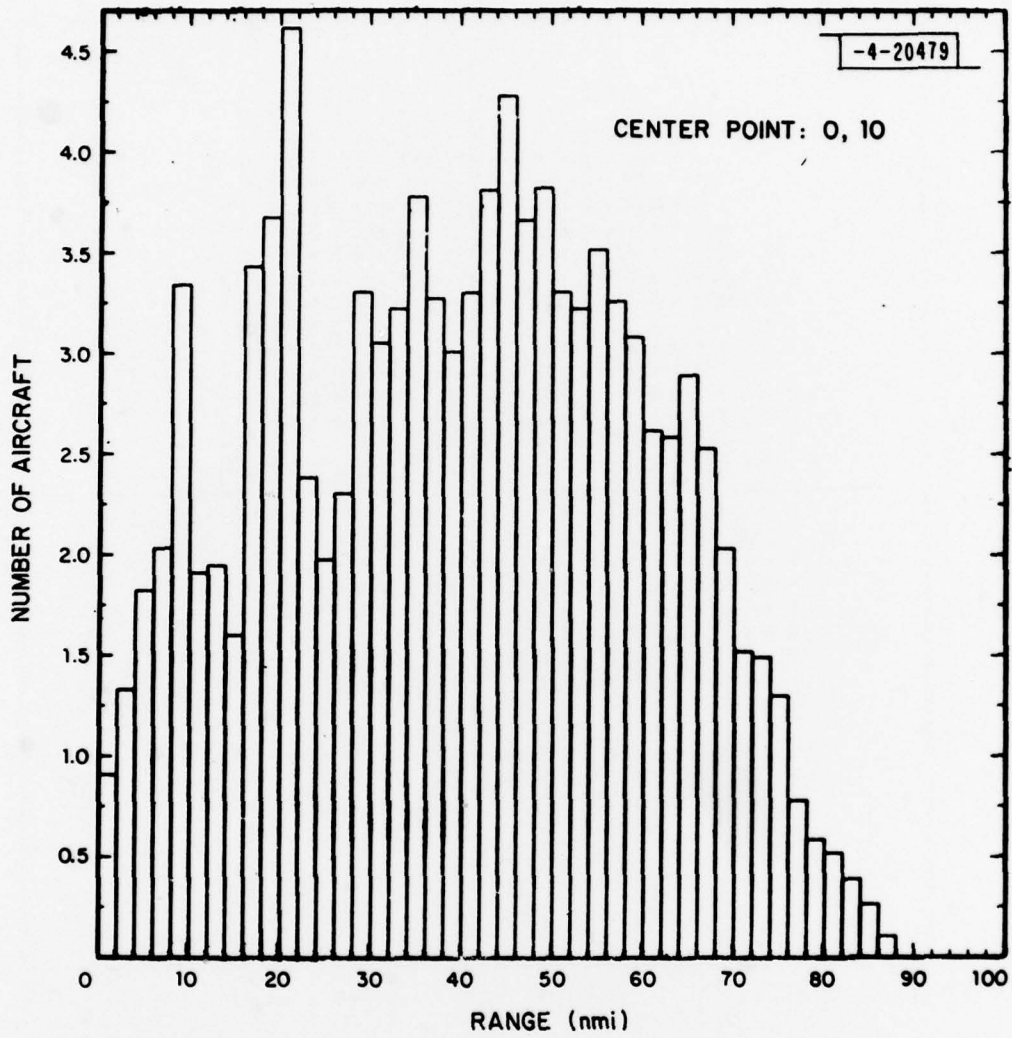


Fig.A-20. Philadelphia histogram, TMF5005

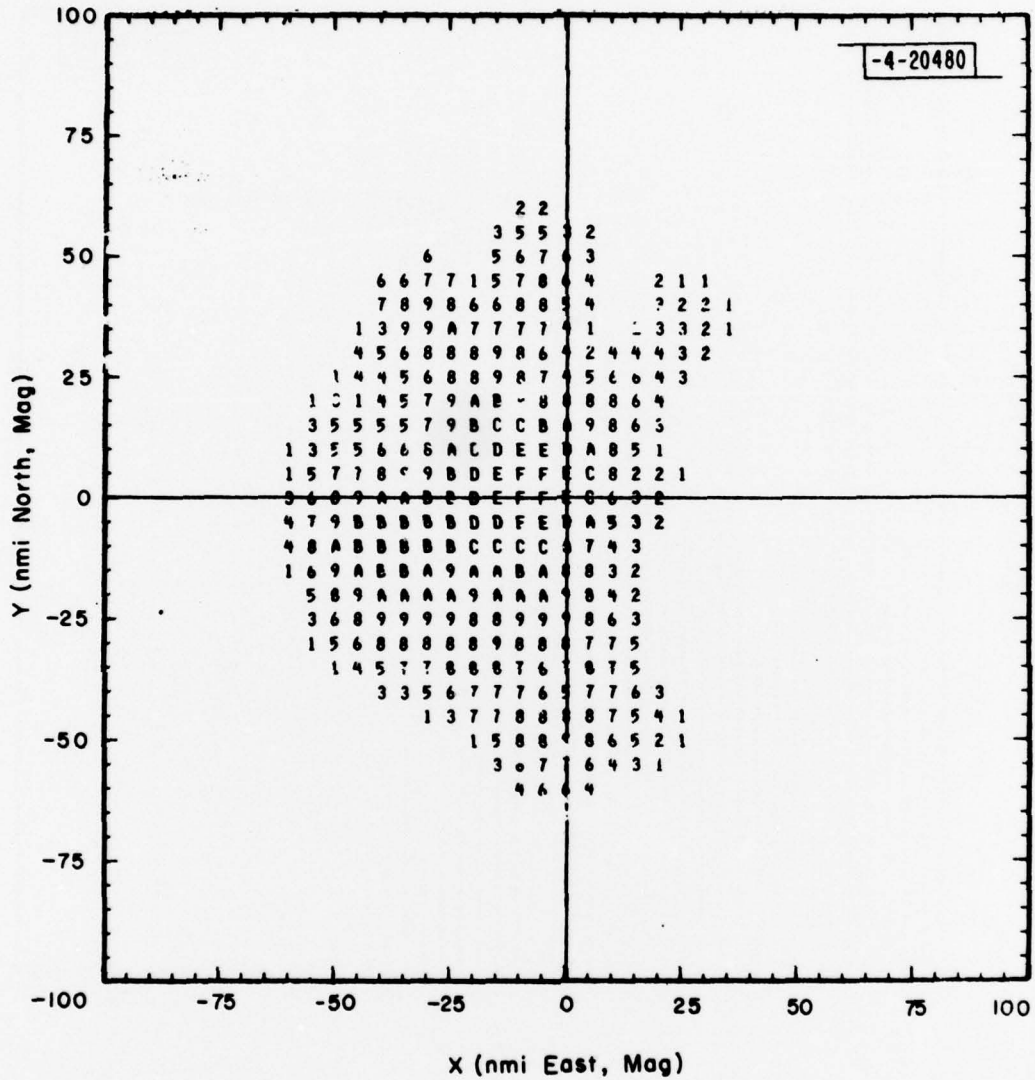


Fig. A-21. Boston map, TMF3031

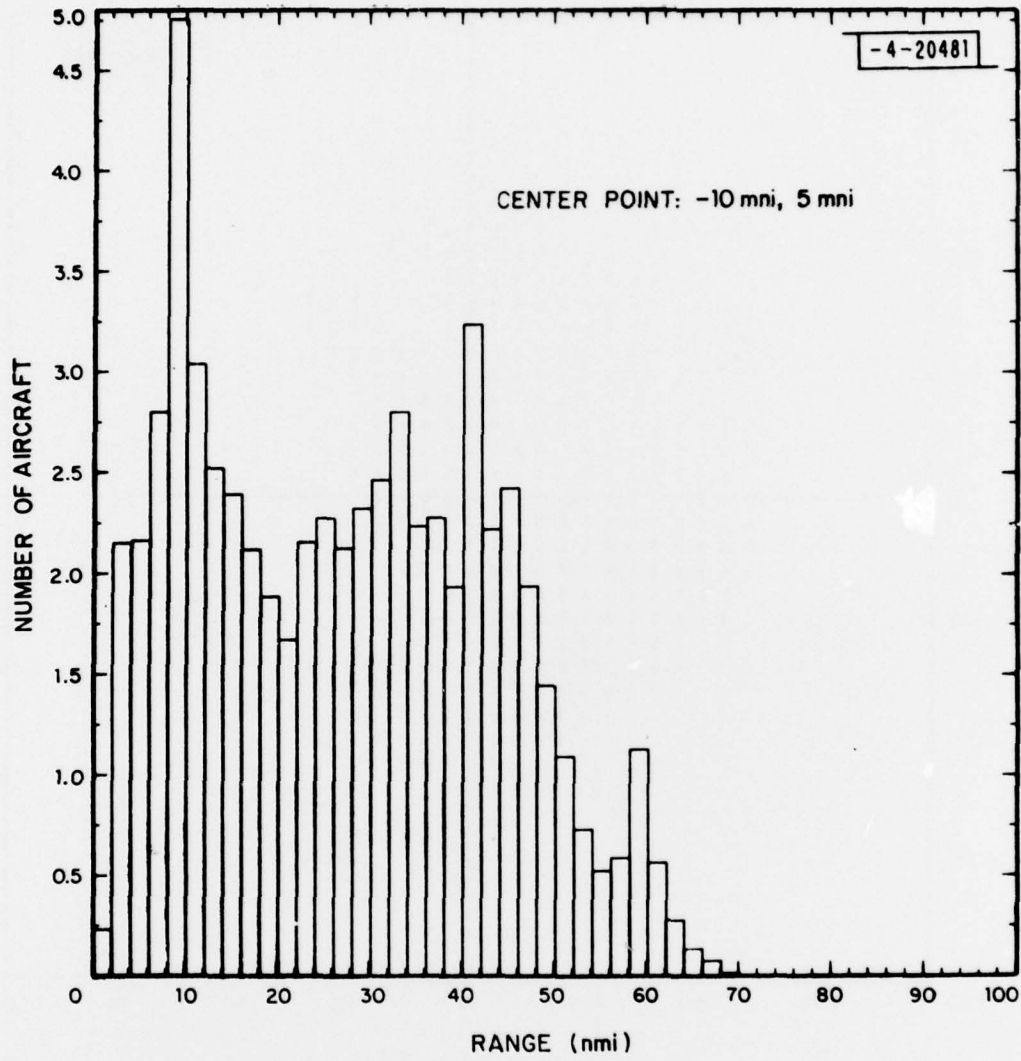


Fig.A-22. Boston histogram, TMF3031

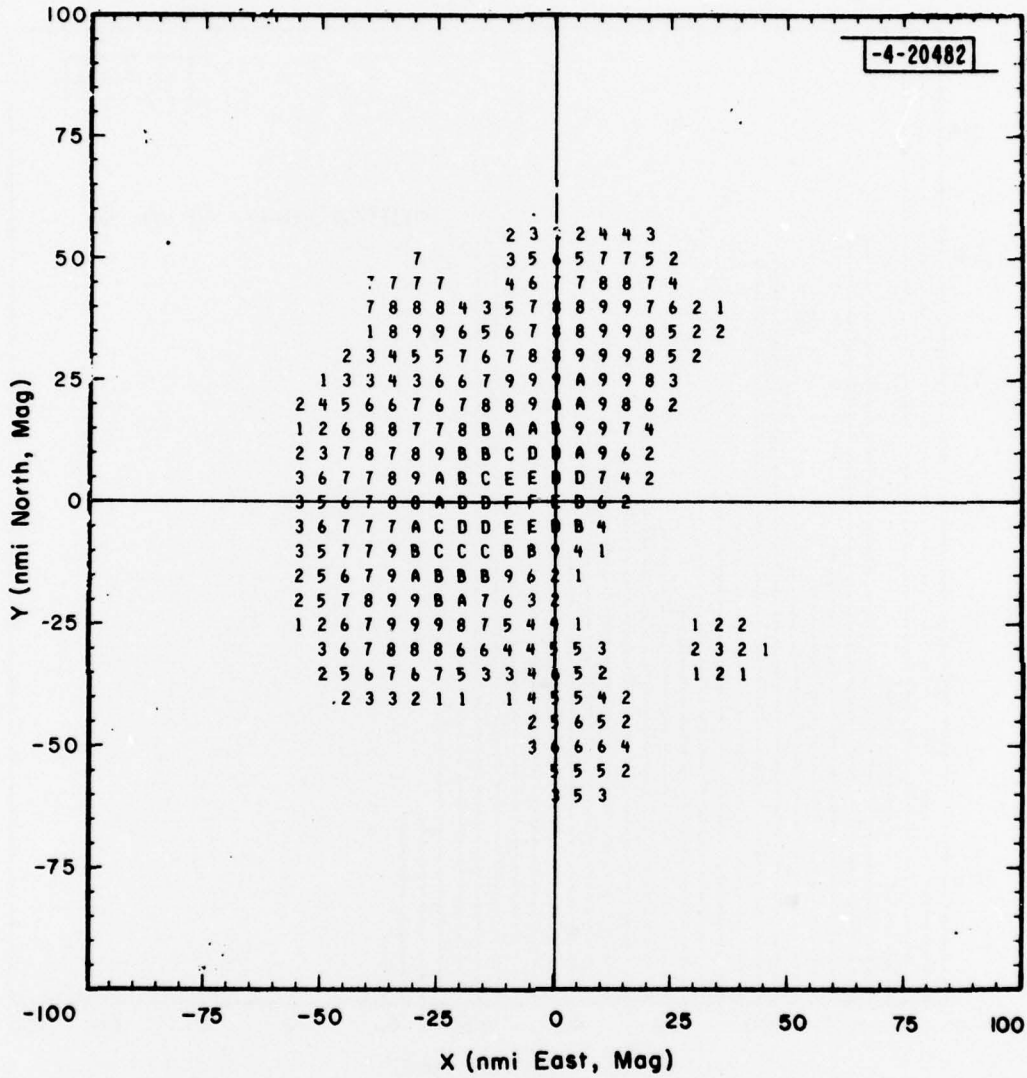


Fig.A-23. Boston map, TMF3037

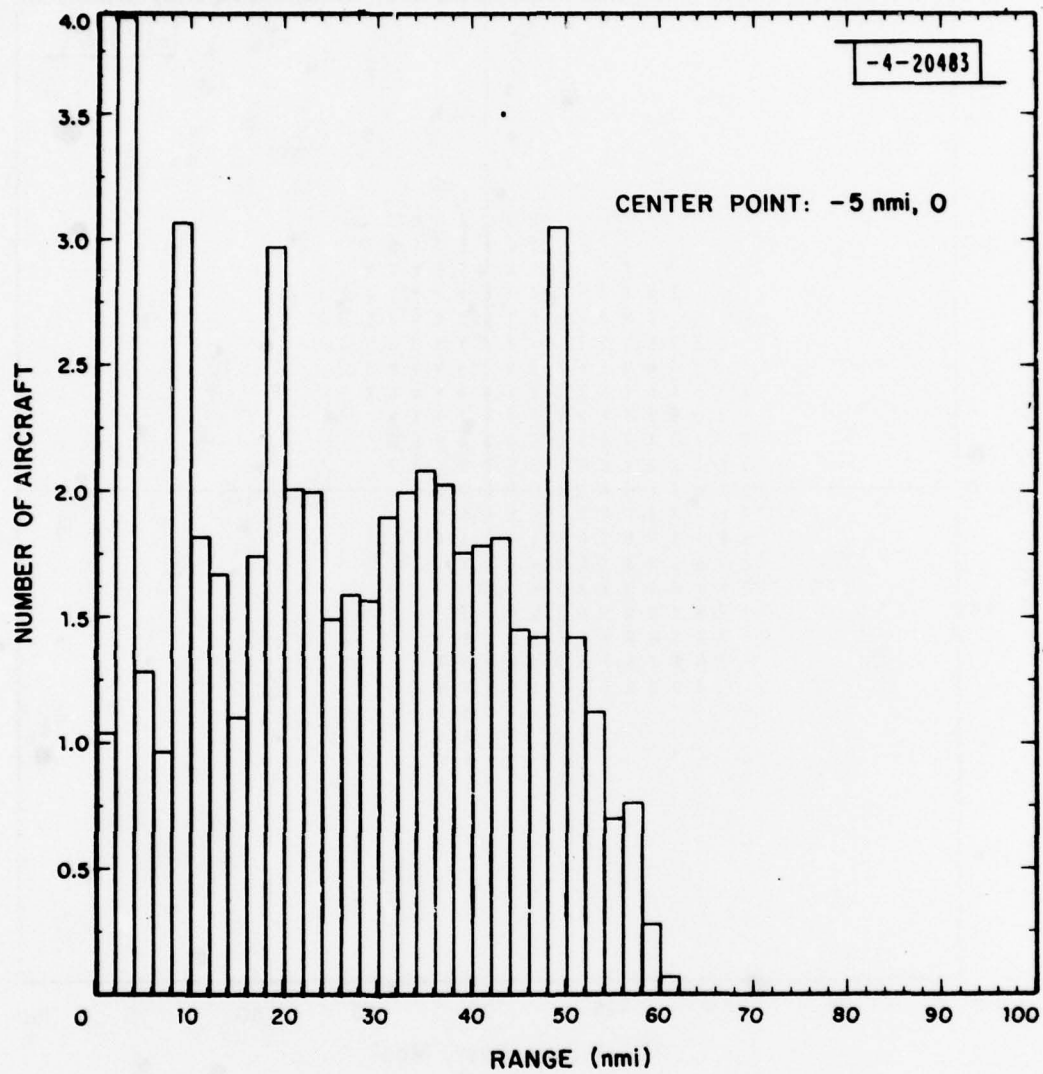


Fig. A-24. Boston histogram, TMF3037

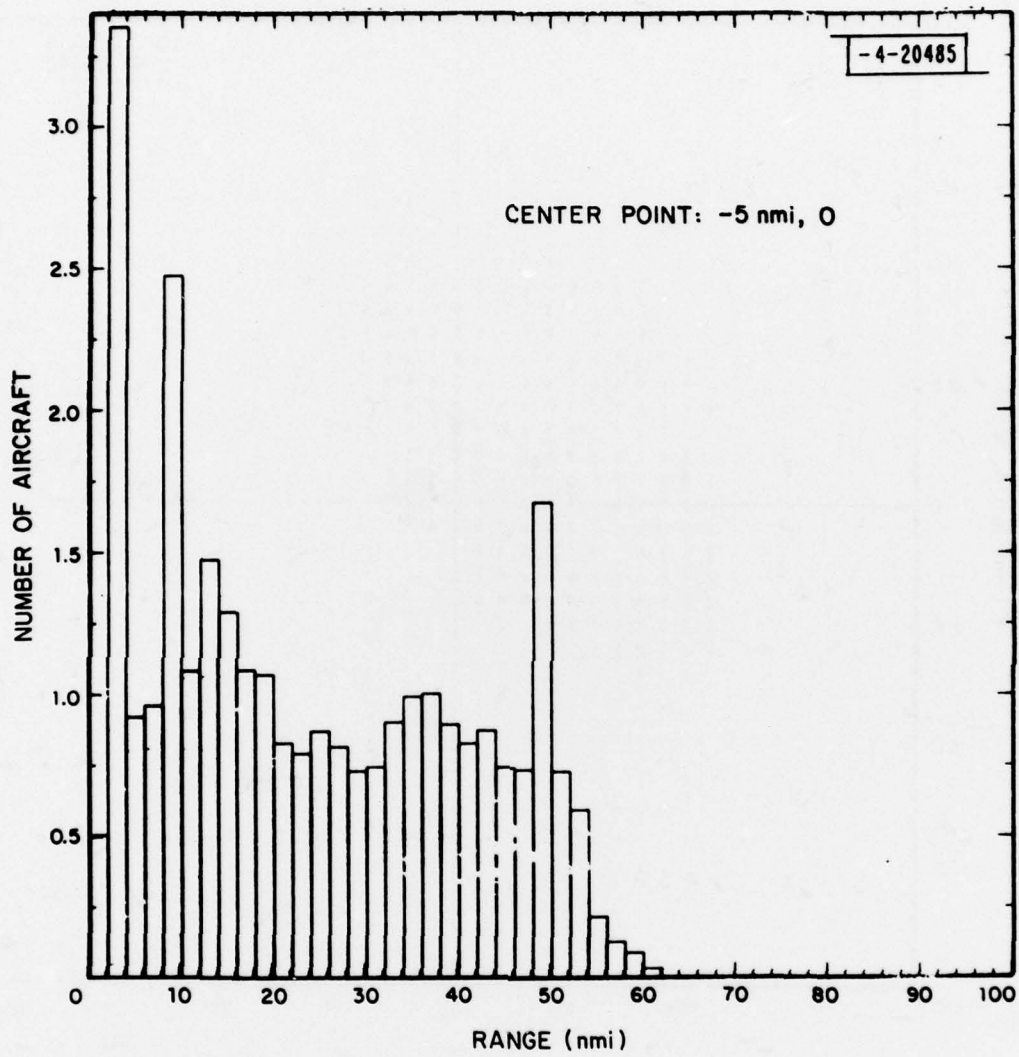


Fig.A-26. Boston histogram, TMF3008